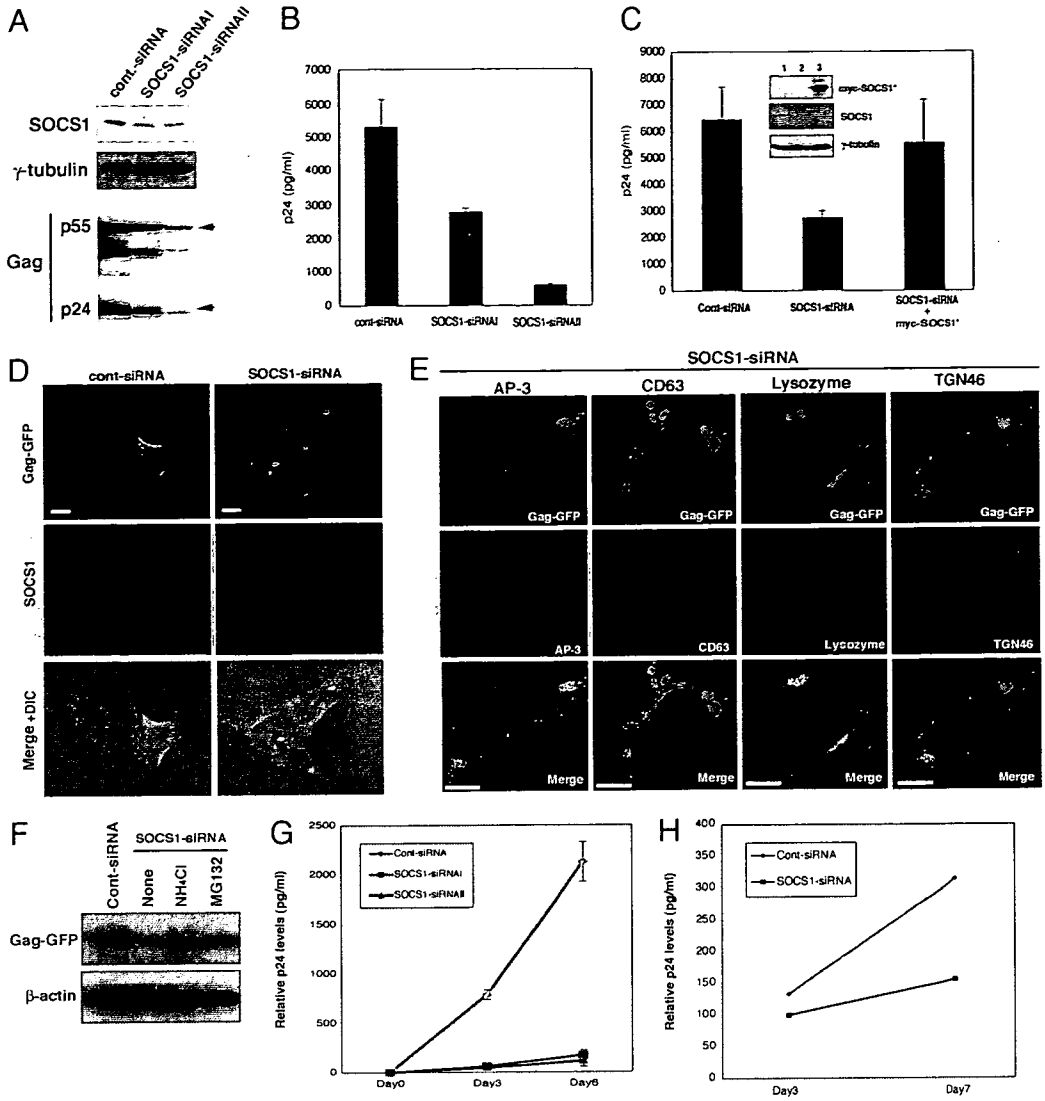

Fig. 4. The targeted inhibition of SOCS1 suppresses Gag trafficking and HIV-1 particle production and enhances Gag degradation in lysosomes. (*A* and *B*) 293T cells were transfected with either control siRNA or two different SOCS1-specific siRNAs (I or II) together with pNL4-3. At 48 h after transfection, cell lysates were subjected to immunoblotting analysis with the indicated antibodies (*A*). Cell supernatants were then subjected to ELISA analysis of p24 levels (*B*). (*C*) 293T cells were transfected with pNL4-3 and cotransfected with control-siRNA, SOCS1-siRNAI alone, or SOCS1-siRNAI plus siRNA-resistant myc-SOCS1 (myc-SOCS1*). After 48 h, cell supernatants were collected and subjected to p24 ELISA. (*Inset*) Immunoblots of the cell lysates. (*D*) HeLa cells were transfected with control or SOCS1-specific siRNA and cotransfected with GFP-Gag. At 48 h after transfection, the cells were subjected to confocal microscopy. (*E*) HeLa cells were transfected with Gag-GFP and SOCS1-siRNA constructs for 48 h. Cells were then fixed and subjected to immunofluorescent analysis with indicated antibodies followed by DAPI staining. (Scale bars: 10 mm.) (*F*) HeLa cells were transfected with Gag-GFP and cotransfected with either control-siRNA or SOCS1-siRNA. After 36 h, the cells were treated with a mock solution, 10 mM NH_4Cl or 10 μM MG132 for another 16 h. Cell were then harvested and subjected to immunoblotting analysis with anti-GFP or anti-β-actin antibodies. (*G*) Jurkat cells were infected with a retroviral vector encoding control (Cont) or two different SOCS1-specific siRNAs (I or II). After selection with puromycin, the cells were then infected with HIV-1_{NL4-3} (multiplicity of infection, 0.1), and p24 antigen levels in cell supernatant were measured by ELISA at the indicated time points. (*H*) Human primary CD4 T cells were separated from healthy donors and infected with lentivirus vectors encoding either control- or SOCS1-siRNAI. The cells were then infected with HIV-1_{NL4-3} (multiplicity of infection, 0.1), and p24 antigen levels in cell supernatant were measured by ELISA at the indicated time points.

this time point, Gag-GFP was found to localize predominantly in a perinuclear region in the control cells (Fig. 3*C*), whereas almost half of the SOCS1-transfected cells exhibited Gag-GFP localization on PM (Fig. 3*D*). These results again indicate that SOCS1 efficiently enhances the trafficking of newly synthesized Gag protein to PM.

The Targeted Disruption of SOCS1 Inhibits Gag Trafficking and HIV-1 Particle Production. To delineate further the role of SOCS1 in the trafficking of Gag and in subsequent HIV-1 particle production, we depleted cellular SOCS1 by siRNA. The significant depletion of SOCS1 expression by two different SOCS1-specific siRNA constructs was confirmed by immunoblotting analysis (Fig. 4 *A* and *B*). Significantly, in cells cotransfected with pNL4-3 and SOCS1-specific siRNAs, both HIV-1 particle release and the levels of intracellular Gag protein are significantly decreased compared with the control cells (Fig. 4 *A* and *B*). Furthermore, the effects of SOCS1-siRNA on the inhibition of HIV-1 particle production was diminished by reexpression with a codon-optimized SOCS1 construct that is resistant to these siRNAs (Fig. 4*C*), indicating that the SOCS1 siRNA suppression of HIV-1 particle production depends on the availability of endogenous SOCS1.

Consistent with these observations, immunofluorescent analysis further revealed that the expression of SOCS1-siRNA dramatically inhibits Gag trafficking such that Gag proteins accumulate in the perinuclear regions as large solid aggregates, as has been reported (20) (Fig. 4*D*). This finding indicates that SOCS1 plays an essential role in the Gag trafficking from perinuclear clusters to PM. Interestingly, these discrete perinuclear clusters of Gag were found to colocalize with lysosome markers, lysozyme, and partly with AP-3, but neither with the late endosome MVB marker CD63 nor the *trans*-Golgi marker TGN46, indicating that Gag is targeted for degradation by lysosomes when the function of SOCS1 is inhibited (Fig. 4*E*). In support of this notion, the levels of intracellular Gag were found to be significantly increased by treatment with a lysosome inhibitor NH_4Cl but not by a proteasome inhibitor MG132 in SOCS1-siRNA cells (Fig. 4*F*), further indicating that the perinuclear clusters of Gag will undergo lysosomal degradation rather than proteasomal degradation when optimal Gag transport to PM is suppressed by the inhibition of SOCS1.

We next addressed whether targeted SOCS1 inhibition would affect HIV-1 particle production in human T cells. The effect of SOCS1 depletion was clearly evident in both HIV-1_{NL4-3}-infected

Jurkat cells and human primary CD4$^+$ T cells, which demonstrated pronounced decreases in virus particle production in SOCS1-siRNA-expressed cells compared with the controls (Fig. 4 *G* and *H*). These results together indicate that the specific inhibition of SOCS1 suppresses the optimal trafficking of Gag to PM, resulting in the degradation of Gag in lysosomes, which in turn leads to the efficient and reproducible inhibition of HIV-1 particle production in various types of human cells.

Discussion

In this work, we report that SOCS1 is an inducible host factor during HIV-1 infection and plays a key role in the late stages of the viral replication pathway via an IFN-independent mechanism (SI Fig. 6). These results represent evidence that SOCS1 is a potent host factor that facilitates HIV-1 particle production via posttranscriptional mechanisms.

SOCS1 has been shown to be a suppressor of several cytokine signaling pathways, and like all SOCS family members it has a central SH2 domain and a conserved C-terminal domain known as the SOCS box (21, 22). Structure–function analyses have further demonstrated that the SOCS1 SH2 domain is required for the efficient binding of its substrates (23, 24). Indeed, our current analyses have also revealed that the SH2 domain of SOCS1 is required for its interaction with the HIV-1 Gag protein. We have shown from our present data that the SOCS box is also required for SOCS1 to function during HIV-1 particle production.

The SOCS box-mediated function of SOCS1 is chiefly exerted via its ubiquitin ligase activity (21, 25). Biochemical binding studies have shown that the SOCS box of SOCS1 interacts with the elongin BC complex, a component of the ubiquitin/proteasome pathway that forms an E3 ligase with Cul2 (or Cul5) and Rbx-1 (21, 26, 27). We show from our current experiments that the SOCS box is required for HIV-1 particle production, indicating the involvement of the ubiquitin/proteasome pathway. However, it is still unknown whether SOCS1 promotes the ubiquitination of Gag and, if so, whether the mono- or poly-ubiquitination of Gag would affect its trafficking and protein stability. Further studies will be necessary to clarify the biological significance of Gag ubiquitination.

Perlman and Resh (20) recently reported that newly synthesized Gag first appears to be diffusely distributed in the cytoplasm, accumulates in perinuclear clusters, passes transiently through a MVB-like compartment, and then traffics to PM. Consistent with these observations, our current work also shows that Gag is accumulated at perinuclear clusters as solid aggregates when its targeting to PM is impaired because of the SOCS1 inhibition.

Another aspect of SOCS1 function during HIV-1 infection was proposed recently. Song *et al.* (28) reported that SOCS1-silenced dendritic cells broadly induce the enhancement of HIV-1 Env-specific CD8$^+$ cytotoxic T lymphocytes and CD4$^+$ T helper cells as well as an antibody response. The induction of the SOCS1 gene in HIV-1 infected cells might therefore disrupt a specific intracellular immune response to HIV-1 in infected host cells.

Based on the strong evidence that we present in our current work that SOCS1 positively regulates the late stages of HIV replication, we conclude that SOCS1 is likely to be a valuable therapeutic target not only for future treatments of AIDS and related diseases, but also for a postexposure prophylaxis against disease in HIV-1-infected individuals.

Materials and Methods

Antibodies and Fluorescent Reagents. Antibodies and fluorescent reagents were obtained from the following sources. Anti-CD63, anti-AP-3, anti-myc (A-14), and anti-SOCS1 (H-93) were from Santa Cruz Biotechnology. Anti-SOCS1 was from Zymed Laboratories. Anti-FLAG (M2) and anti-HA (12CA5) were from Sigma and Roche Diagnostics, respectively. Anti-HIV-p24 (Dako; Cytomation), anti-STAT1, and anti-phospho-STAT1 (Y701) were from BD Transduction Laboratories. Sheep polyclonal anti-TGN46 was from GeneTex.

Plasmid Constructs. Expression constructs for SOCS1 have been described in ref. 29. GST fusion constructs with specific regions derived from the codon-optimized *gag* were generated (MA, CA, NC, p6, Δp6, full-length Gag) by cloning into pGEX-2T (GE Healthcare Bio-Sciences) as described in ref. 30. For retrovirus-mediated siRNA expression, pSUPER.retro.puro vector was digested, as described in ref. 31, with the following sequences: SOCS1-siRNAI, TCGAGCTGCTGGAGCACTA; SOCS1-siRNAII, GGCCAGAACCTTCCTCCTCTT; control siRNA, TCGTATGTTGTGTGGAATT.

Electron Microscopy. Transfected 293T cells were fixed with 2.5% glutaraldehyde and subjected to TEM, as described (14, 32).

ACKNOWLEDGMENTS. We thank Dr. H Gottlinger (University of Massachusetts) for providing plasmids. This work was supported in part by grants from the Ministry of Education, Culture, Sports, Science, and Technology of Japan and Human Health Science of Japan.

1. Sorin M, Kalpana GV (2006) *Curr HIV Res* 4:117–130.
2. Freed EO (2004) *Trends Microbiol* 12:170–177.
3. Peterlin BM, Trono D (2003) *Nat Rev Immunol* 3:97–107.
4. Trkola A (2004) *Curr Opin Microbiol* 7:555–559.
5. Freed EO (1998) *Virology* 251:1–15.
6. Adamson CS, Jones IM (2004) *Rev Med Virol* 14:107–121.
7. VerPlank L, Bouamr F, LaGrassa TJ, Agresta B, Kikonyogo A, Leis J, Carter CA (2001) *Proc Natl Acad Sci USA* 98:7724–7729.
8. Garrus JE, von Schwedler UK, Pornillos OW, Morham SG, Zavitz KH, Wang HE, Wettstein DA, Stray KM, Cote M, Rich RL, *et al.* (2001) *Cell* 107:55–65.
9. Strack B, Calistri A, Craig S, Popova E, Gottlinger HG (2003) *Cell* 114:689–699.
10. Dong X, Li H, Derdowski A, Ding L, Burnett A, Chen X, Peters TR, Dermody TS, Woodruff E, Wang JJ, *et al.* (2005) *Cell* 120:663–674.
11. Alroy I, Tuvia S, Greener T, Gordon D, Barr HM, Taglicht D, Mandil-Levin R, Ben-Avraham D, Konforty D, Nir A, *et al.* (2005) *Proc Natl Acad Sci USA* 102:1478–1483.
12. Ryo A, Suzuki Y, Ichiyama K, Wakatsuki T, Kondoh N, Hada A, Yamamoto M, Yamamoto N (1999) *FEBS Lett* 462:182–186.
13. Adachi A, Gendelman HE, Koenig S, Folks T, Willey R, Rabson A, Martin MA (1986) *J Virol* 59:284–291.
14. Demirov DG, Ono A, Orenstein JM, Freed EO (2002) *Proc Natl Acad Sci USA* 99:955–960.
15. Chang TL, Mosoian A, Pine R, Klotman ME, Moore JP (2002) *J Virol* 76:569–581.
16. De Sepulveda P, Okkenhaug K, Rose JL, Hawley RG, Dubreuil P, Rottapel R (1999) *EMBO J* 18:904–915.
17. Kamio M, Yoshida T, Ogata H, Douchi T, Nagata Y, Inoue M, Hasegawa M, Yonemitsu Y, Yoshimura A (2004) *Oncogene* 23:3107–3115.
18. Gallina A, Mantoan G, Rindi G, Milanesi G (1994) *Biochem Biophys Res Commun* 204:1031–1038.
19. Accola MA, Strack B, Gottlinger HG (2000) *J Virol* 74:5395–5402.
20. Perlman M, Resh MD (2006) *Traffic* 7:731–745.
21. Alexander WS (2002) *Nat Rev Immunol* 2:410–416.
22. Marine JC, Topham DJ, McKay C, Wang D, Parganas E, Stravopodis D, Yoshimura A, Ihle JN (1999) *Cell* 98:609–616.
23. Narazaki M, Fujimoto M, Matsumoto T, Morita Y, Saito H, Kajita T, Yoshizaki K, Naka T, Kishimoto T (1998) *Proc Natl Acad Sci USA* 95:13130–13134.
24. Yasukawa H, Misawa H, Sakamoto H, Masuhara M, Sasaki A, Wakioka T, Ohtsuka S, Imaizumi T, Matsuda T, Ihle JN, *et al.* (1999) *EMBO J* 18:1309–1320.
25. Tyers M, Rottapel R (1999) *Proc Natl Acad Sci USA* 96:12230–12232.
26. Kamizono S, Hanada T, Yasukawa H, Minoguchi S, Kato R, Minoguchi M, Hattori K, Hatakeyama S, Yada M, Morita S, *et al.* (2001) *J Biol Chem* 276:12530–12538.
27. Kamura T, Burian D, Yan Q, Schmidt SL, Lane WS, Querido E, Branton PE, Shilatifard A, Conaway RC, Conaway JW (2001) *J Biol Chem* 276:29748–29753.
28. Song XT, Evel-Kabler K, Rollins L, Aldrich M, Gao F, Huang XF, Chen SY (2006) *PLoS Med* 3:e11.
29. Ryo A, Suizu F, Yoshida Y, Perrem K, Liou YC, Wulf G, Rottapel R, Yamaoka S, Lu KP (2003) *Mol Cell* 12:1413–1426.
30. Morikawa Y, Kishi T, Zhang WH, Nermut MV, Hockley DJ, Jones IM (1995) *J Virol* 69:4519–4523.
31. Ryo A, Uemura H, Ishiguro H, Saitoh T, Yamaguchi A, Perrem K, Kubota Y, Lu KP, Aoki I (2005) *Clin Cancer Res* 11:7523–7531.
32. Nagashima Y, Nishihira H, Miyagi Y, Tanaka Y, Sasaki Y, Nishi T, Imaizumi K, Aoki I, Misugi K (1996) *Cancer* 77:799–804.

MAJOR ARTICLE

Interleukin-4–Transgenic hu-PBL-SCID Mice: A Model for the Screening of Antiviral Drugs and Immunotherapeutic Agents against X4 HIV-1 Viruses

Kazu Okuma,[1] Reiko Tanaka,[1] Tomoyuki Ogura,[2] Mamoru Ito,[2] Sei Kumakura,[3] Mikiro Yanaka,[3] Masako Nishizawa,[4] Wataru Sugiura,[4] Naoki Yamamoto,[4] and Yuetsu Tanaka[1]

[1]Department of Immunology, Graduate School and Faculty of Medicine, University of the Ryukyus, Okinawa, [2]Central Institute for Experimental Animals, Kanagawa, and [3]Kureha Corporation and [4]National Institute of Infectious Diseases, Tokyo, Japan

CXCR4-tropic (X4) human immunodeficiency virus type 1 (HIV-1) does not efficiently infect and replicate in severe combined immunodeficiency (SCID) mice reconstituted with human peripheral blood mononuclear cells, termed "hu-PBL-SCID mice," due to, at least in part, relatively low levels of expression of the CXCR4 coreceptor. To overcome this limitation, interleukin (IL)–4–transgenic hu-PBL-SCID mice were derived that spontaneously synthesized human IL-4, which has been shown to enhance CXCR4 expression and promote X4 virus infection in vitro. Experiments reported here show that (1) synthesis of human IL-4 in vivo augmented CXCR4 expression on human CD4$^+$ lymphocytes and importantly led to productive infection of not only X4 HIV-1_{NL4-3} but also multidrug-resistant primary clinical isolates and that (2) the in vivo infection could be significantly blocked by the administration of a CXCR4 antagonist. Altogether, IL-4–transgenic hu-PBL-SCID mice provide a useful model for X4 HIV-1 study and testing/screening of anti-X4 viral drugs.

HIV-1 isolates enter target cells primarily after binding to the CD4 receptor and via the CXCR4 and CCR5 coreceptors [1–5] and are classified into X4 and R5 strains, respectively [6]. The X4 isolates are frequently implicated in the decline of peripheral CD4$^+$ T cell counts characteristic of the late stage of HIV-1 infection proceeding to the development of AIDS [7].

hu-PBL-SCID mice have been extensively used as a small animal model to study HIV-1 pathogenesis [8–14]. Results from a previous study showed that, although infection of human peripheral blood mononuclear cell (PBMC)–reconstituted hu-PBL-SCID mice with a predominantly R5 HIV-1 caused intensive CD4$^+$ T cell depletion, infection of similarly reconstituted mice with the same infectious dose of an X4 HIV-1 resulted in little or no CD4$^+$ T cell depletion [11]. Thereafter, it was noted that this limitation of X4 HIV-1 infection was due, at least in part, to a decrease in the intensity of CXCR4 expression on CD4$^+$ T cells [13]. Thus, it was reasoned that the pathogenic effects of the X4 HIV-1 strains in the hu-PBL-SCID mice might be related to the relative levels of the expression of HIV-1 coreceptor (the state of activation/differentiation) on human CD4$^+$ T cells at the time of infection in these mice. This limitation has to date restricted our ability to use this mouse model for understanding the mechanisms of X4 HIV-1 pathogenesis and for the evaluation of candidate therapeutics against X4 viruses. These findings prompted us to seek alternative strategies for the development of an improved hu-PBL-SCID mouse system that is permissive for infection/replication of X4 isolates.

Human interleukin (IL)–4 has been shown to specifically enhance the cell-surface expression of CXCR4 on

Received 1 May 2007; accepted 11 July 2007; electronically published 4 December 2007.

Potential conflicts of interest: none reported.

Presented in part: First International Workshop on Humanized Mice, Tokyo, 11–12 October 2006 (abstract P-15); 14th Conference on Retroviruses and Opportunistic Infections, Los Angeles, 25–28 February 2007 (abstract 496).

Financial support: Health and Labor Science Research Grant (Research on Publicly Essential Drugs and Medical Devices) from the Ministry of Health, Labor, and Welfare of Japan (grant H16-soyaku-004).

Reprints or correspondence: Dr. Kazu Okuma, Dept. of Immunology, Graduate School and Faculty of Medicine, University of the Ryukyus, Uehara 207, Nishihara-cho, Nakagami-gun, Okinawa 903-0215, Japan (kokuma@med.u-ryukyu.ac.jp).

The Journal of Infectious Diseases 2008; 197:134–41

0022-1899/2008/19701-0021$15.00
DOI: 10.1086/524303

resting peripheral blood T cells [15]. Furthermore, it has been reported that human IL-4 plays an important role in rendering $CD4^+$ T cells susceptible to X4 HIV-1 infection via enhanced cell-surface expression of the CXCR4 coreceptor in vitro [15–17].

In efforts to overcome the limitation inherent with the use of hu-PBL-SCID mice for the study of X4 HIV-1 as described above, we developed an IL-4–transgenic immunodeficient mouse model that consistently secreted readily detectable serum levels of human IL-4. We show here that X4 isolates readily infect/replicate in this mouse model but not in wild-type (wt) non–IL-4–transgenic mice and that this model can now be exploited for the rapid evaluation of the therapeutic efficacy of new anti-X4 HIV-1 agents in vivo.

METHODS

IL-4–producing mice. Two strains of human IL-4–transgenic immunodeficient mice were bred on the C.B-17-*scid* [18] and BALB/cA-Rag2$^{-/-}\gamma_c^{-/-}$ (dKO) genetic background mice [19, 20] at the Central Institute for Experimental Animals (CIEA) as follows. PBMCs were isolated from a healthy human volunteer and activated in vitro with pokeweed mitogen. RNA was prepared from these PBMCs, and then cDNA was synthesized by reverse-transcriptase polymerase chain reaction (PCR). Human IL-4 cDNA was amplified from the cDNA using one set of primers: 5'-CCCGGGATCGTTAGCTTCTCCTGATAAAA-3' and 5'-GCGGCCGCTATTCAGCTCGAACACTTTGAAT-3'. The product was inserted into the PCR2.1 vector by use of the TA cloning kit (Invitrogen) and the insert sequenced. After confirmation of the sequence, IL-4 cDNA was inserted into pCMVb with a CMV promoter (Invitrogen). To produce transgenic mice, a DNA fragment containing the CMV promoter, IL-4 cDNA, and Poly(A) regions was excised with *Xho*I and *Hind*III sites of pCMVb and microinjected into the pronuclei of fertilized eggs from the 2 strains (C.B-17-*scid* and BALB/cA-dKO) of mice. These eggs were subsequently transplanted into oviducts of pseudopregnant foster recipient mice. The offspring mice were screened to confirm the insertion of the transgene into the genome by PCR, and serum from these mice was screened for levels of human IL-4 by ELISA with a commercial kit (BD). The IL-4 transgene–hemizygous mice were maintained by mating them with wt mice with the same genetic background in the specific-pathogen–free (SPF) facility of the CIEA. The mice were transferred to the SPF and biosafety level 3 facilities of the Institute for Animal Experiments, University of the Ryukyus, and were used for further experiments. The experimental protocols were approved by the Institutional Animal Care and Use Committee on the basis of the Regulation for Animal Experimentation of the CIEA and University of the Ryukyus before the initiation of the study.

Viruses. X4 HIV-1_{NL4-3} was obtained as described elsewhere [14]. Fourteen multidrug-resistant (MDR) HIV-1 clinical isolates were obtained from HIV-1–infected patients who had been treated with highly active antiretroviral therapy (HAART). The viruses were propagated in PBMCs stimulated with phytohemagglutinin (PHA; Sigma), IL-2 (National Institutes of Health AIDS Research and Reference Reagent Program), and IL-4 (Peprotec). Three isolates from these MDR isolates that efficiently grew in the activated cells were selected for further experiments. The titers of virus stocks were determined by end-point titration using a 2-fold limiting dilution of the stock and in vitro PHA-activated human PBMCs, and the infectious units (IU) were calculated.

CXCR4 antagonist. The synthesis and purification of the CXCR4 antagonist KRH-1636 were performed at Kureha Corporation as described elsewhere [21]. As a control, the carrier tartrate was used in parallel.

Transplantation and infection. The control (wt) and the IL-4–transgenic C.B-17-*scid* mice were depleted of NK cells by the intraperitoneal (ip) injection of 0.5–1.0 mg of anti–mouse IL-2R β (TMβ-1) [22] per animal. The IL-4–transgenic and the control BALB/cA-dKO mice do not require TMβ-1 treatment because they lack NK cells [19, 20]. PBMCs were isolated from healthy human donors. Groups of 2–4-month-old IL-4–transgenic mice from each of the 2 background strains and their corresponding non–IL-4–transgenic wt mice were injected ip with PBMCs 3 days later. Groups of mice were challenged 24 h later ip with mock, HIV-1_{NL4-3}, or MDR isolates (2000 IU/500 μL/animal). For the experiments using the CXCR4 antagonist, groups of mice were administered 0.1 mL of 10 mmol/L KRH-1636, the tartrate carrier or saline ip at 1 h before and 1 day after virus infection. At 6–8 days after infection, the mice were killed, their blood was obtained by cardiocentesis, and human lymphocytes were collected from the peritoneal lavage fluids. The serum samples were assayed for levels of human IL-4 by use of an ELISA kit (R&D Systems). The human lymphocytes were analyzed using flow cytometry as described below. The remaining cells were cultured in RPMI 1640 medium (Sigma) supplemented with fetal calf serum and IL-2. The peritoneal lavage fluids, serum samples, and lymphocyte culture supernatants were examined for levels of p24 by use of an ELISA kit (Zepto Metrix).

Flow cytometry analysis. Cell samples to be analyzed by flow cytometry were initially incubated with normal human IgG for blocking of the Fc receptors. For cell-surface staining, aliquots of cells were then stained with Cy5-labeled anti-CD4 (OKT4) and phycoerythrin-labeled anti-CXCR4 (12G5; Dako) or with Cy5-labeled anti-CD3 (OKT3). For intracellular staining, after CD3 staining the aliquots of cells were fixed, permeabilized, and incubated with fluorescein isothiocyanate–labeled anti–HIV-1 Gag p24 (2C2; Y.T. et al., unpublished data). Stained samples were analyzed on a FACSCalibur flow cytometer, using Cell Quest software (BD Pharmingen). Aliquots of cells stained

Table 1. Expression of human CD4, CXCR4, and intracellular HIV-1 p24 in cells from X4 HIV-1–infected hu-PBL-SCID mice.

Category	X4 HIV-1 infection	Mice, no.	$CD4^+$ T cells, %	*P*	$CXCR4^+CD4^+$ T cells, %	*P*	$p24^+$ T cells, %	*P*
C.B-17-*scid* mice								
Control	NL4-3	6	22.1 ± 8.3	<.001	45.2 ± 4.7	<.001	0.1 ± 0.1	NS
IL-4 transgenic	NL4-3	6	66.3 ± 9.0		65.5 ± 6.1		0.1 ± 0.1	
BALB/cA-dKO mice								
Control	NL4-3	5	35.9 ± 5.1	<.01	32.6 ± 1.4	<.001	0.2 ± 0.1	<.05
IL-4 transgenic	NL4-3	3	57.4 ± 8.3		68.2 ± 3.9		3.2 ± 1.2	

NOTE. Cells in peritoneal lavage fluid from control and interleukin (IL)–4–transgenic hu-PBL-SCID mice on either the C.B-17-*scid* or BALB/cA-dKO background were labeled with appropriate monoclonal antibodies and analyzed by flow cytometry, as described in Methods. Analyzed data are shown as mean ± SD values. NS, not significant. The indicated *P* values for the comparison of control vs. transgenic mice for each category are based on Student's *t* test.

with or without each of the antibodies described above were used as controls for the purposes of establishing gates and for the determination of the frequency of positive cells.

Statistical analysis. Data obtained by flow cytometry were analyzed by Student's *t* test with GraphPad Prism (version 4.0c for Mac OS X; GraphPad Software).

RESULTS

Production of human IL-4 in IL-4–transgenic mice. Efforts to construct the IL-4–transgenic mice constitutively synthesizing human IL-4 finally led to the establishment of mice on each of the 2 immunodeficient backgrounds expressing either high or low serum levels of human IL-4 (data not shown). On the basis of preliminary data obtained on the efficiency of virus replication, all subsequent experiments were done using only the 2 strains with high serum IL-4 expression levels. We assayed for levels of human IL-4 in the serum from the $IL\text{-}4^+$ hu-PBL-SCID mice and the wt hu-PBL-SCID mice on either the C.B-17-*scid* or BALB/cA-dKO background after infection with X4 HIV-$1_{NL4\text{-}3}$. Serum from each of the IL-4–transgenic mice on either background contained significant levels of human IL-4 (~800–1800 pg/mL), whereas serum from the control mice on the same background showed nondetectable levels of human IL-4. These data demonstrate that the human IL-4 synthesized by the IL-4–transgenic mice is generated from the transgene but not from the human PBMCs transplanted in these mice.

Effect of human IL-4 on the levels of human CXCR4 and CD4 expression by cells transplanted into mice. Since human IL-4 has been previously documented to enhance the expression of CXCR4 in vitro, experiments were done to examine the expression of human CXCR4 on transplanted $CD4^+$ cells in the peritoneal lavage fluids from HIV-$1_{NL4\text{-}3}$–infected $IL\text{-}4^+$ hu-PBL-SCID mice and control hu-PBL-SCID mice on either the C.B-17-*scid* or BALB/cA-dKO background. There did not appear to be any detectable difference in the absolute amounts of cells recovered from the peritoneal lavage fluids from the IL-4–positive or IL-4–negative hu-PBL-SCID mice on either background (data not shown). Flow cytometry analysis demonstrated that the frequency of human $CD4^+$ cells from the IL-4–transgenic C.B-17-*scid* or BALB/cA-dKO mice was significantly higher than that from the control mice (table 1). As expected, there was a marked increase in the frequency of CXCR4-expressing $CD4^+$ cells from the IL-4–transgenic mice on either genetic background relative to that from the control mice (figure 1*A* and table 1). Thus, these data indicate that human IL-4 produced endogenously is functional in vivo in terms of its ability to enhance human CXCR4 expression on $CD4^+$ cells transplanted into the mice.

Increased frequency of X4 HIV-1–infected cells from IL-4–transgenic hu-PBL-SCID mice. Since the constitutive synthesis of human IL-4 in IL-4–transgenic hu-PBL-SCID mice resulted in the enhanced expression of X4 HIV-1 receptors (human CXCR4/CD4) on the transplanted cells, we reasoned that such cells were likely to be more permissive to the infection and replication of X4 HIV-1. We thus challenged the IL-4–transgenic hu-PBL-SCID mice and control hu-PBL-SCID mice bred on the C.B-17-*scid* or BALB/cA-dKO mice with HIV-$1_{NL4\text{-}3}$. Cells obtained from the peritoneal lavage fluids were analyzed for cell-surface expression of human CD3 (since HIV-1 downmodulates CD4 expression) and the presence of intracellular p24. As seen in figure 1*B* and table 1, although very few if any $CD3^+$ cells from the control or IL-4–transgenic C.B-17-*scid* mice showed p24 expression, there was a >10-fold increase in the frequency of $CD3^+$ T cells that expressed p24 from the IL-4–transgenic BALB/cA-dKO mice relative to the control mice. These data suggest that, while transgene-induced human IL-4 increases the frequency of $CD4^+CXCR4^+$ T cells transplanted into both the C.B-17-*scid* and the BALB/cA-dKO mice, only the latter demonstrates increased sensitivity to X4 HIV-1 infection and replication, at least when this assay is used (see below).

High production of X4 HIV-1 in the culture supernatants of cells from IL-4–transgenic hu-PBL-SCID mice. In an effort

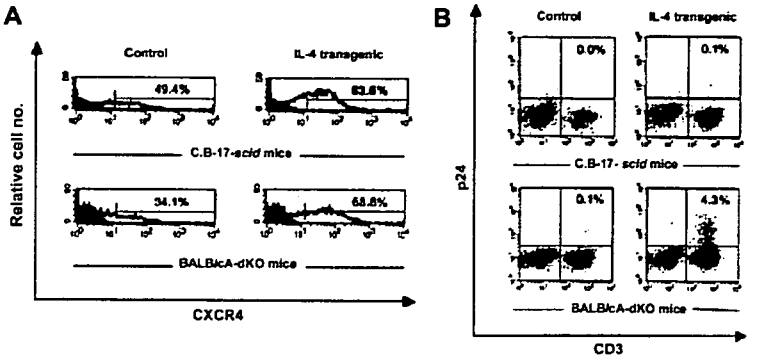

Figure 1. Enhancement of the expression of CXCR4 coreceptor and facilitation of X4 HIV-1 infection and replication in hu-PBL-SCID mice by in vivo production of human interleukin (IL)–4. Groups of hu-PBL-SCID mice, generated from IL-4–transgenic and nontransgenic (control) mice on either the C.B-17-*scid* or BALB/cA-dKO background, were injected intraperitoneally with HIV-1_{NL4-3} at −24 h after peripheral blood mononuclear cell (PBMC) reconstitution. Six to eight days later, peritoneal lavage fluids were harvested from mice in each group, and cells were collected from the fluids by density-gradient centrifugation. *A*, Cells analyzed for the frequency and mean density of human CXCR4 expression on $CD4^+$ cells by flow cytometry. Data for analyzed cells are depicted by a thick line, and the background control profile is depicted by a thin line and gray shading. The nos. above the bars represent the percentage of positive cells. Data shown are representative of mice in each group from 3 independent experiments. *B*, HIV-1 infectivity. Cells were subjected to flow cytometry after cell-surface CD3 and intracellular p24 staining. Analyzed data are depicted as dot plots. The nos. in the graphs indicate the percentage of $CD3^+p24^+$ cells. Data displayed are representative of mice in each group from 3 independent experiments.

to determine the reason for our failure to detect levels of intracellular p24 in the IL-4–transgenic mice on the C.B-17-*scid* background and to further support the above finding, peritoneal lavage fluids were collected from mock- or HIV-1_{NL4-3}–infected $IL\text{-}4^+$ hu-PBL-SCID mice and, for purposes of control, the HIV-1_{NL4-3}–infected non–IL-4–transgenic mice on the C.B-17-*scid* background. The cells were isolated from the peritoneal lavage fluids, and an aliquot was analyzed for the frequency and the relative density of human CXCR4/CD4; the remaining aliquot was cultured in vitro. In addition, the peritoneal lavage fluids and the culture supernatants of cells at days 1–3 after culture were assayed for levels of p24 production. As displayed in table 2, although the frequency of $CXCR4^+CD4^+$ cells in the IL-4–transgenic mice was significantly higher than that in the nontransgenic mice, the mean fluorescence intensity (MFI) of CXCR4 expressed by the $CD4^+$ T cells from these mice was not increased compared with the control (because of an increase in the frequency of $CXCR4^+CD4^+$ cells with relatively low MFI; see figure 1*A*). Analysis of levels of synthesized p24 demonstrated marked differences, as shown in figure 2. Thus, although the amounts of p24 produced were modest in the peritoneal lavage fluids and the cell-culture supernatants from HIV-1–infected control mice, the levels of p24 produced by those from HIV-1–infected IL-4–transgenic mice were strikingly higher (15,429, 11,844, 1696, and 53 pg/mL in the supernatants on day 3) (mean, 48.9 vs. 7255 pg/mL; >100-fold increase). Although the levels of p24 produced by one of the IL-4–transgenic mice (mouse 12) were similar to those in the control mice, this was likely due to the much lower relative level of human IL-4 (354 pg/mL in serum) produced by mouse 12 than those from the other 3 IL-4–transgenic mice (4227, 6313, and 2356 pg/mL in serum). The present data not only document the fact that the cells from these

Table 2. Effect of the CXCR4 antagonist KRH-1636 on the expression of human CXCR4 by $CD4^+$ cells from X4 HIV-1–infected interleukin (IL)–4–transgenic hu-PBL-SCID mice.

C.B-17-*scid* mice	X4 HIV-1 Infection	CXCR4 antagonist	Mice, no.	$CXCR4^+CD4^+$ T cells, %	*P*	CXCR4 on $CD4^+$ T cells, MFI	*P*
Control	NL4-3	Mock	4	45.5 ± 9.3	<.05[a]	73.7 ± 36.0	NS[a]
IL-4 transgenic	NL4-3	Mock	4	66.7 ± 7.4	NS[b]	73.1 ± 6.2	<.05[b]
IL-4 transgenic	NL4-3	KRH-1636	4	63.0 ± 4.2	...	62.2 ± 4.8	...

NOTE. Control or IL-4–transgenic hu-PBL-SCID mice on the C.B-17-*scid* background infected with X4 HIV-1_{NL4-3} were administered mock KRH-1636 or real KRH-1636. Cells isolated from the peritoneal lavage fluid from the mice in each group were labeled with appropriate monoclonal antibodies and subjected to flow cytometry, as described in Methods. Data analyzed are displayed as mean ± SD values. MFI, mean fluorescence intensity; NS, not significant. The indicated *P* values are based on Student's *t* test.

[a] For the comparison between control mice and IL-4–transgenic mice that received a mock CXCR4 antagonist.

[b] For the comparison between IL-4–transgenic mice that received a mock CXCR4 antagonist and IL-4–transgenic mice that received KRH-1636.

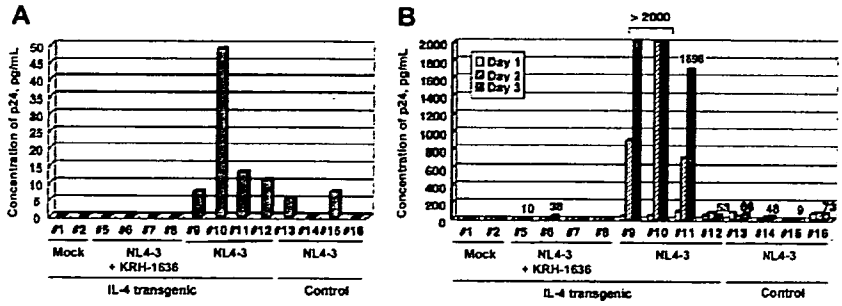

Figure 2. Efficient infection of interleukin (IL)–4–producing hu-PBL-SCID mice with X4 laboratory strain and an inhibitory effect of the CXCR4 antagonist KRH-1636 on infection. Twelve IL-4–transgenic and 4 nontransgenic (control) hu-PBL-SCID mice were generated on the C.B-17-*scid* background. Among them, 8 IL-4–transgenic and 4 control mice were infected intraperitoneally (ip) with the X4 laboratory strain (HIV-1_{NL4-3}) and 4 IL-4–transgenic mice were mock-infected at 1 day after engraftment. To evaluate the effect of KRH-1636, this drug was administered ip twice, at 1 h before and 1 day after infection of 4 IL-4–transgenic mice (NL4-3 + KRH-1636). At 8 days after infection, peritoneal lavage fluids were obtained from the mice in each group. Cells were isolated from the fluids and cultured in IL-2–containing medium. Levels of HIV-1 p24 in the peritoneal lavage fluids *(A)* and culture supernatants at days 1–3 after incubation *(B)* were quantitated for infectivity and replication efficiency by ELISA. With regard to the data on mock-infected mice, only 2 of 4 representative data are presented. The nos. listed above the bars in the graph indicate levels of HIV-1 p24 when it was detectable on day 3 (most of the values were <200 pg/mL, and select samples showed values of >2000 pg/mL). Pound signs (#) indicate mouse nos. Results shown are representative of 3 independent experiments.

IL-4–transgenic C.B-17-*scid* mice are susceptible but also demonstrate that the virus from such cells is replication competent. In addition, these findings suggest that the use of intracellular p24 levels is not a sensitive enough technique and that data using the intracellular p24 assay need to be carefully evaluated. These data also indicate that the IL-4–transgenic hu-PBL-SCID mice provide a powerful model for the study of X4 HIV-1 infection independently of the genetic background of the mice.

Inhibitory effect of the CXCR4 antagonist on infection of IL-4–transgenic hu-PBL-SCID mice with the X4 laboratory strain. In an effort to further validate that the CXCR4 coreceptor was indeed used by the X4 HIV-1 virus in the IL-4–transgenic hu-PBL-SCID mice, we used the X4 virus-entry inhibitor, CXCR4 antagonist KRH-1636. Thus, the IL-4–transgenic hu-PBL-SCID mice on the C.B-17-*scid* background were infected with X4 laboratory strain HIV-1_{NL4-3} and were either mock treated or treated with KRH-1636, and the peritoneal lavage fluids, cells in fluids, and cell-culture supernatants were examined as described above. As shown in table 2, the frequency of $CXCR4^+CD4^+$ cells in KRH-1636–treated IL-4–transgenic mice was marginally lower than that in mock-treated IL-4–transgenic mice. In addition, the MFI of CXCR4 expression by the $CD4^+$ T cells was clearly reduced by KRH-1636 administration. Importantly, treatment with KRH-1636 almost completely blocked X4 HIV-1 infection in these IL-4–transgenic mice (figure 2). These data indicate that X4 HIV-1 infection in transgenic mice is CXCR4 dependent and that our mouse model can be used to develop and test new anti-X4 HIV-1 drugs in vivo.

Therapeutic effect of KRH-1636 on the infection of IL-4–transgenic hu-PBL-SCID mice with MDR clinical isolates. The appearance of MDR HIV-1 clinical isolates has been and continues to be one of the growing problems in a significant number of patients receiving HAART and seriously limits the use of the antiviral drugs that are currently available. Thus, the development of novel adjunct or alternative therapeutics is an urgent need. Since treated patients tend to harbor significantly higher levels of either dual/mixed or X4 viruses [23] and since MDR isolates are not usually refractory to new treatment with drugs from classes that have not been used previously in patients from which the viruses were derived, we finally wanted to examine the effect of KRH-1636 on MDR HIV-1 infection in IL-4–transgenic hu-PBL-SCID mice. For this experiment, we used the IL-4–transgenic BALB/cA-dKO mice instead of the IL-4–transgenic C.B-17-*scid* mice, because the former seems more permissive to X4 HIV-1 infection than the latter, as described above. Before the in vivo study, we confirmed that the in vitro infection by 3 MDR clinical isolates could be inhibited with KRH-1636 (more than ~90% inhibition at the 5-μmol/L level). Thus, groups of IL-4–transgenic hu-PBL-SCID mice were infected with a mixture of these selected MDR isolates containing equal IU of each virus and treated with KRH-1636 or the tartrate carrier control. Thereafter, the cells obtained from the peritoneal lavage fluids were analyzed for the expression of cell-surface human CD4, CD3, and intracellular p24. The serum, peritoneal lavage fluids, and supernatants following in vitro culture of the cells for 24 h were assayed for levels of p24 production. Flow cytometry analysis after CD4 staining demonstrated a significant decline in $CD4^+$ T cells in 2 (mouse 7 and mouse 8) of 4 control-treated mice (figure 3*A*; top profile shows data from 1 of these 2 mice), which was likely due to MDR HIV-1 pathogenesis. However, importantly, no detectable depletion of $CD4^+$ T cells was observed in any of 4 KRH-1636–treated mice (figure 3*A*; bottom profile). As summarized in table 3, the difference in the frequency of $CD4^+$ T cells between the control-treated mice and the

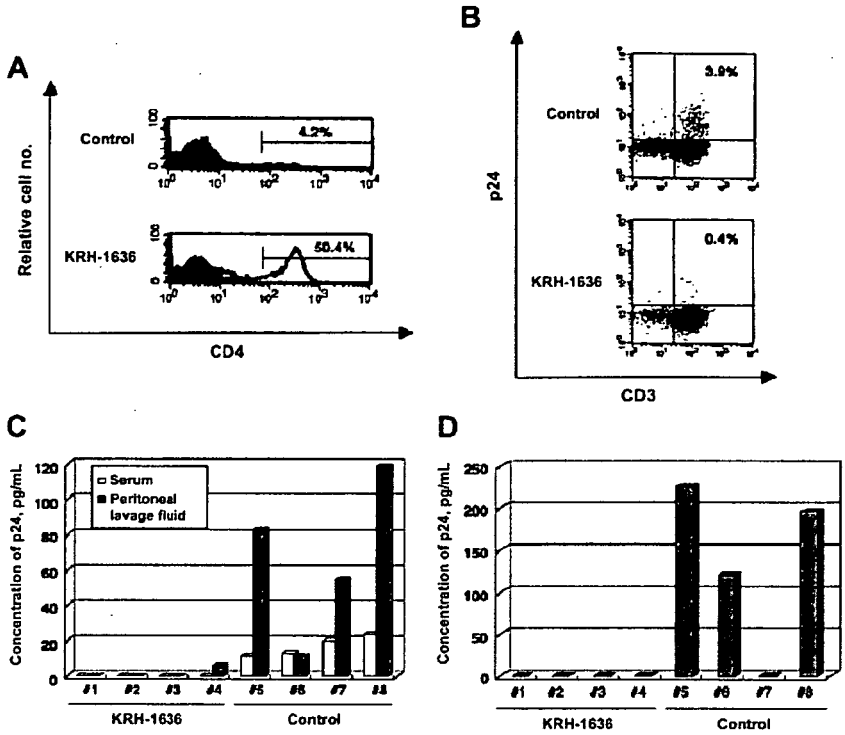

Figure 3. Prophylactic effect of KRH-1636 on infection and pathogenesis by multidrug-resistant (MDR) HIV-1 clinical isolates. Eight interleukin (IL)–4–transgenic hu-PBL-SCID mice (BALB/cA-dKO) were infected intraperitoneally (ip) with a mixture of MDR HIV-1 clinical isolates at 1 day after human peripheral blood mononuclear cell transfer. In an effort to assess the effect of KRH-1636 on HIV-1 infection, this agent or tartrate (control drug) was administered to 4 mice per group ip twice, at 1 h before infection and 1 day after infection. At 7 days after infection, serum and peritoneal lavage fluids were harvested from mice in each group, and cells were collected from the fluids. *A*, Cells examined for human CD4 expression by cell-surface staining and standard flow cytometry. Representative data from a single mouse from the control-treated or the KRH-1636–treated HIV-1–infected mice are shown. The frequency of $CD4^+$ T cells is depicted by a thick line, and the background control is depicted by a thin line with gray shading. The nos. above the bars indicate the percentage of positive cells. *B*, Aliquot of the peritoneal lavage cells analyzed by flow cytometry for the frequency of $CD3^+$ T cells that were positive for the intracellular presence of HIV-1 p24. Representative data of cells from the control-treated and the KRH-1636–treated HIV-1–infected mice are shown. The nos. in the graphs indicate the percentage of $CD3^+p24^+$ cells. *C*, Concentrations of p24 in serum and peritoneal lavage fluid. Concentrations were determined by ELISA to quantify MDR HIV-1 infection and replication efficiency. Pound signs (#) indicate mouse nos. *D*, Levels of in vitro p24 production. The remaining cells were cultured in a microtiter plate containing $IL\text{-}2^+$ medium for ~24 h, and the culture supernatants obtained were assayed for levels of in vitro p24 production by ELISA. Pound signs (#) indicate mouse nos. Results shown are representative of 3 similar independent experiments.

KRH-1636–treated mice was not significant. However, the MFI of CD4 expression was significantly decreased in the control-treated mice (229.3 vs. 296.3; $P < .05$). Results of CD3/p24 staining showed that the frequency of $CD3^+p24^+$ cells was markedly inhibited in the KRH-1636–treated mice, compared with that in the carrier-treated control mice (figure 3*B* and table 3). Furthermore, levels of HIV-1 p24 in the serum samples, peritoneal lavage fluids, and culture supernatants from the KRH-

Table 3. Effect of KRH-1636 on infection and pathogenesis by multidrug-resistant (MDR) HIV-1 clinical isolates in interleukin (IL)–4–transgenic hu-PBL-SCID mice.

BALB/cA-dKO mice	X4 HIV-1 infection	CXCR4 antagonist	Mice, no.	$CD4^+$ T cells, %	*P*	$CD4^+$ T cells, MFI	*P*	$p24^+$ T cells, %	*P*
IL-4 transgenic	MDR	Control	4	14.7 ± 11.9	NS	229.3 ± 33.0	<.05	3.2 ± 0.8	<.01
IL-4 transgenic	MDR	KRH-1636	4	31.3 ± 15.7		296.3 ± 25.2		0.8 ± 0.7	

NOTE. IL-4–transgenic hu-PBL-SCID mice on the BALB/cA-dKO background were infected with MDR HIV-1 clinical isolates and administered tartrate (control) or KRH-1636. Cells in peritoneal lavage fluid from the mice in each group were stained with appropriate monoclonal antibodies and analyzed by flow cytometry, as described in Methods. Data shown here are mean ± SD values. MFI, mean fluorescence intensity; NS, not significant. The indicated *P* values for the comparison between control mice and mice that received KRH-1636 are based on Student's *t* test.

1636–treated HIV-1–infected mice were almost completely reduced relative to those in the control mice (figure 3*C* and 3*D*). Note that the failure to detect the in vitro production of p24 in mouse 7 might result from depletion of $CD4^+$ T cells (figure 3*D*). These data demonstrate that the CXCR4 antagonist KRH-1636 has a marked degree of prophylactic effect on infection with pathogenic MDR clinical isolates in vivo.

DISCUSSION

Humanized mice that have served as valuable small animal models include the SCID-hu Thy/Liv mouse [24–28]. This mouse model, generated by implanting human hematopoietic tissues (human fetal thymus/liver) under the kidney capsule, has been used for the study of HIV-1 and is known for permissiveness to X4 HIV-1 infection [26–28]. However, the use of this model is limited by the fact that the implants are of human fetal organ origins that are not easily available. On the other hand, the hu-PBL-SCID mouse model provides another surrogate in vivo HIV-1 infection assay system. Although this model has led to a number of successful studies of HIV-1 [8–14], there was still a limitation in that it was difficult to demonstrate X4 HIV-1 infection and replication in such mice. Thus, to add extra value to the use of this mouse system for the study of HIV-1, in the present study we developed novel human IL-4–transgenic hu-PBL-SCID mice that enable CXCR4-using HIV-1 strains to efficiently infect and replicate in these mice.

Human IL-4 has low homology with murine IL-4 both at the gene and protein levels, accounting for the lack of cross-reactivity of this cytokine in the 2 species in vitro [29–32]. Results of the experiments reported here indicate that the high efficiency of X4 HIV-1 infection in the IL-4–transgenic hu-PBL-SCID mice was, at least in part, secondary to enhanced expression of viral receptors induced by human IL-4 synthesized endogenously. Interestingly, although there was no apparent increase in the number of cells recovered from the engrafted transgenic mice, there was a significant increase in the number of $CD4^+$ T cells recovered (1.5–3-fold). It is thus possible that the other cell lineages migrate from the peritoneal cavity to other tissues of the mice, resulting in enrichment of the $CD4^+$ T cell lineage. However, further studies of other tissues are needed to clarify this issue. Furthermore, our preliminary experiments indicate that the IL-4–transgenic hu-PBL-SCID mice remain permissive to R5 strain infection (data not shown).

In this report, we created 2 types of novel hu-PBL-SCID mice by transplanting human PBMCs into IL-4–transgenic C.B-17-*scid* and BALB/cA-dKO mice. The data obtained show that hu-PBL-SCID mice using the IL-4–producing BALB/cA-dKO mice appeared more permissive to X4 HIV-1 infection than did those using the IL-4–producing C.B-17-*scid* mice, at least as determined by the presence of intracellular p24. Although the reasons for this difference remain to be determined, it should be noted that, whereas the BALB/cA-dKO mice were derived by double mutation with defects in both the recombinase-activating gene 2 (Rag-2) and the gene encoding the γ_c chain of select cytokine receptors [19, 20], the C.B-17-*scid* mice have only the Rag-2 mutation [18]. Thus, although the Rag-2 mutation prevents the normal maturation of T and B lymphocytes, the γ_c chain mutation abrogates the expression of functional receptors for IL-2 and other cytokines, preventing the expansion of lymphocytes, including NK cells, which play an important role in the innate immune response such as nonspecific rejection of xenogeneic grafts. It is thus possible that the C.B-17-*scid* mice maintain a low but significant residual level of NK cell function, which may play a role in the difference noted above even though they were administered significant levels of anti–IL-2Rβ antibody. Since the BALB/cA-dKO mice are completely deficient in NK cell lineage and function, they are more immunodeficient than the C.B-17-*scid* mice, suggesting that the level and type of immunodeficiency in the BALB/cA-dKO mice may facilitate better engraftment and more efficient viral infection and propagation within these mice. These select defects of the BALB/cA-dKO mice might render the IL-4–transgenic mouse model on this background more valuable and ideal for studies of X4 HIV-1.

Acknowledgments

We thank the National Institutes of Health AIDS Research and Reference Reagent Program and M. Sasaki for supplying interleukin-2 and technical support, respectively. We are also grateful to Prof. Aftab Ansari for his critical reading of the manuscript and for his helpful discussion about and suggestions for the manuscript.

References

1. Feng Y, Broder CC, Kennedy PE, Berger EA. HIV-1 entry cofactor: functional cDNA cloning of a seven-transmembrane, G protein-coupled receptor. Science **1996**; 272:872–7.
2. Alkhatib G, Combadiere C, Broder CC, et al. CC CKR5: a RANTES, MIP-1alpha, MIP-1beta receptor as a fusion cofactor for macrophage-tropic HIV-1. Science **1996**; 272:1955–8.
3. Berson JF, Long D, Doranz BJ, Rucker J, Jirik FR, Doms RW. A seven-transmembrane domain receptor involved in fusion and entry of T-cell-tropic human immunodeficiency virus type 1 strains. J Virol **1996**; 70: 6288–95.
4. Deng H, Liu R, Ellmeier W, et al. Identification of a major co-receptor for primary isolates of HIV-1. Nature **1996**; 381:661–6.
5. Doranz BJ, Rucker J, Yi Y, et al. A dual-tropic primary HIV-1 isolate that uses fusin and the beta-chemokine receptors CKR-5, CKR-3, and CKR-2b as fusion cofactors. Cell **1996**; 85:1149–58.
6. Berger EA, Doms RW, Fenyo EM, et al. A new classification for HIV-1. Nature **1998**; 391:240.
7. Xiao L, Rudolph DL, Owen SM, Spira TJ, Lal RB. Adaptation to promiscuous usage of CC and CXC-chemokine coreceptors in vivo correlates with HIV-1 disease progression. AIDS **1998**; 12:F137–43.
8. Mosier DE. Adoptive transfer of human lymphoid cells to severely immunodeficient mice: models for normal human immune function, autoimmunity, lymphomagenesis, and AIDS. Adv Immunol **1991**; 50:303–25.
9. Mosier DE, Gulizia RJ, Baird SM, Wilson DB, Spector DH, Spector SA. Human immunodeficiency virus infection of human-PBL-SCID mice. Science **1991**; 251:791–4.

10. Torbett BE, Picchio G, Mosier DE. hu-PBL-SCID mice: a model for human immune function, AIDS, and lymphomagenesis. Immunol Rev **1991**; 124:139–64.
11. Mosier DE, Gulizia RJ, MacIsaac PD, Torbett BE, Levy JA. Rapid loss of CD4+ T cells in human-PBL-SCID mice by noncytopathic HIV isolates. Science **1993**; 260:689–92.
12. Rizza P, Santini SM, Logozzi MA, et al. T-cell dysfunctions in hu-PBL-SCID mice infected with human immunodeficiency virus (HIV) shortly after reconstitution: in vivo effects of HIV on highly activated human immune cells. J Virol **1996**; 70:7958–64.
13. Fais S, Lapenta C, Santini SM, et al. Human immunodeficiency virus type 1 strains R5 and X4 induce different pathogenic effects in hu-PBL-SCID mice, depending on the state of activation/differentiation of human target cells at the time of primary infection. J Virol **1999**; 73:6453–9.
14. Yoshida A, Tanaka R, Murakami T, et al. Induction of protective immune responses against R5 human immunodeficiency virus type 1 (HIV-1) infection in hu-PBL-SCID mice by intrasplenic immunization with HIV-1-pulsed dendritic cells: possible involvement of a novel factor of human CD4+ T-cell origin. J Virol **2003**; 77:8719–28.
15. Jourdan P, Abbal C, Noraz N, et al. IL-4 induces functional cell-surface expression of CXCR4 on human T cells. J Immunol **1998**; 160:4153–7.
16. Tanaka Y, Koyanagi Y, Tanaka R, Kumazawa Y, Nishimura T, Yamamoto N. Productive and lytic infection of human CD4+ type 1 helper T cells with macrophage-tropic human immunodeficiency virus type 1. J Virol **1997**; 71:465–70.
17. Suzuki Y, Koyanagi Y, Tanaka Y, et al. Determinant in human immunodeficiency virus type 1 for efficient replication under cytokine-induced CD4+ T-helper 1 (Th1)- and Th2-type conditions. J Virol **1999**; 73:316–24.
18. Bosma GC, Custer RP, Bosma MJ. A severe combined immunodeficiency mutation in the mouse. Nature **1983**; 301:527–30.
19. Traggiai E, Chicha L, Mazzucchelli L, et al. Development of a human adaptive immune system in cord blood cell-transplanted mice. Science **2004**; 304:104–7.
20. Berges BK, Wheat WH, Palmer BE, Connick E, Akkina R. HIV-1 infection and CD4 T cell depletion in the humanized Rag2$^{-/-}\gamma c^{-/-}$ (RAG-hu) mouse model. Retrovirology **2006**; 3:76.
21. Ichiyama K, Yokoyama-Kumakura S, Tanaka Y, et al. A duodenally absorbable CXC chemokine receptor 4 antagonist, KRH-1636, exhibits a potent and selective anti-HIV-1 activity. Proc Natl Acad Sci USA **2003**; 100:4185–90.
22. Tanaka T, Kitamura F, Nagasaka Y, Kuida K, Suwa H, Miyasaka M. Selective long-term elimination of natural killer cells in vivo by an anti-interleukin 2 receptor beta chain monoclonal antibody in mice. J Exp Med **1993**; 178:1103–7.
23. Hunt PW, Harrigan PR, Huang W, et al. Prevalence of CXCR4 tropism among antiretroviral-treated HIV-1–infected patients with detectable viremia. J Infect Dis **2006**; 194:926–30.
24. Goldstein H, Pettoello-Mantovani M, Katopodis NF, Kim A, Yurasov S, Kollmann TR. SCID-hu mice: a model for studying disseminated HIV infection. Semin Immunol **1996**; 8:223–31.
25. McCune JM. Animal models of HIV-1 disease. Science **1997**; 278:2141–2.
26. Aldrovandi GM, Feuer G, Gao L, et al. The SCID-hu mouse as a model for HIV-1 infection. Nature **1993**; 363:732–6.
27. Berkowitz RD, Alexander S, Bare C, et al. CCR5- and CXCR4-utilizing strains of human immunodeficiency virus type 1 exhibit differential tropism and pathogenesis in vivo. J Virol **1998**; 72:10108–17.
28. Bonyhadi ML, Rabin L, Salimi S, et al. HIV induces thymus depletion in vivo. Nature **1993**; 363:728–32.
29. Yokota T, Otsuka T, Mosmann T, et al. Isolation and characterization of a human interleukin cDNA clone, homologous to mouse B-cell stimulatory factor 1, that expresses B-cell- and T-cell-stimulating activities. Proc Natl Acad Sci USA **1986**; 83:5894–8.
30. Bonsch D, Kammer W, Lischke A, Friedrich K. Species-specific agonist/antagonist activities of human interleukin-4 variants suggest distinct ligand binding properties of human and murine common receptor gamma chain. J Biol Chem **1995**; 270:8452–7.
31. Idzerda RL, March CJ, Mosley B, et al. Human interleukin 4 receptor confers biological responsiveness and defines a novel receptor superfamily. J Exp Med **1990**; 171:861–73.
32. Morrison BW, Leder P. A receptor binding domain of mouse interleukin-4 defined by a solid-phase binding assay and in vitro mutagenesis. J Biol Chem **1992**; 267:11957–63.

JOURNAL OF VIROLOGY, Dec. 2007, p. 13259–13264
0022-538X/07/$08.00+0 doi:10.1128/JVI.01353-07

Vol. 81, No. 23

Humanized NOD/SCID/IL2Rγ^{null} Mice Transplanted with Hematopoietic Stem Cells under Nonmyeloablative Conditions Show Prolonged Life Spans and Allow Detailed Analysis of Human Immunodeficiency Virus Type 1 Pathogenesis▽

Satoru Watanabe,[1,2] Shinrai Ohta,[3] Misako Yajima,[4] Kazuo Terashima,[5] Mamoru Ito,[6] Hideo Mugishima,[7] Shigeyoshi Fujiwara,[4] Kazufumi Shimizu,[2] Mitsuo Honda,[3] Norio Shimizu,[1]* and Naoki Yamamoto[3,5]*

Department of Virology, Division of Medical Science, Medical Research Institute, Tokyo Medical and Dental University, 1-5-45 Yushima, Bunkyo-ku, Tokyo 113-8519, Japan[1]; Open Research Center for Genome and Infectious Disease Control, Nihon University School of Medicine, 30-1 Oyaguchikami-chou, Itabashi-ku, Tokyo 173-8610, Japan[2]; AIDS Research Center, National Institute of Infectious Diseases, 1-23-1 Toyama, Shinjuku-ku, Tokyo 162-8640, Japan[3]; Department of Infectious Diseases, National Research Institute for Child Health and Development, 2-10-1 Okura, Setagaya-ku, Tokyo 154-8567, Japan[4]; Department of Molecular Virology, Graduate School of Medicine, Tokyo Medical and Dental University, 1-5-45 Yushima, Bunkyo-ku, Tokyo 113-8519, Japan[5]; Central Institute for Experimental Animals, 1430 Nogawa, Miyamae-ku, Kawasaki, Kanagawa 216-0001, Japan[6]; and Department of Pediatrics and Child Health, Nihon University School of Medicine, 30-1 Oyaguchikami-chou, Itabashi-ku, Tokyo 173-8610, Japan[7]

Received 21 June 2007/Accepted 3 September 2007

In a previous study, we demonstrated that humanized NOD/SCID/IL2Rγ^{null} (hNOG) mice constructed with human hematopoietic stem cells (HSCs) allow efficient human immunodeficiency virus type 1 (HIV-1) infection. However, HIV-1 infection could be monitored for only 43 days in the animals due to their short life spans. By transplanting HSCs without any myeloablation methods, the mice successfully survived longer than 300 days with stable engraftment of human cells. The mice showed high viremia state for more than the 3 months examined, with systemic HIV-1 infection and gradual decrease of CD4$^+$ T cells analogous to that in humans. These capacities of the hNOG mice are very attractive for modeling mechanisms of AIDS progression and therapeutic strategy.

One of the main problems in the field of human immunodeficiency virus type 1 (HIV-1) research is the lack of suitable small animal models for studying the virological and pathogenic aspects of human HIV-1 infection. To overcome the drawback that HIV-1 does not replicate in rodent cells, severe combined immunodeficiency (SCID) mice, engrafted with human peripheral blood mononuclear cells (hu-PBL-SCID) (16) or human fetal thymus and liver tissue [SCID-hu (Thy/Liv)] (18), have been used for the small animal models of HIV-1 infection. However, these mouse models fall short of accurately mirroring human HIV infection because of their short infection spans (17), limited infection of lymphoid tissues (15), and partial infection to coreceptor tropic HIVs (4, 10, 13).

Considering the significant advantages of developing a mouse model for HIV-1 infection, we previously introduced a novel HIV-1 mouse model using nonobese diabetic (NOD)/SCID/interleukin-2 receptor (IL-2R) gamma chain-knocked-out (NOG) mice (22). Multilineage human cells, including T, B, NK cells, monocytes/macrophages, and dendritic cells (DCs) differentiate in the mice when transplanted with human CD34$^+$ hematopoietic stem cells (HSCs) (6, 9, 22). These mice show high levels of susceptibility to both CCR5 (R5)- and CXCR4 (X4)-tropic HIVs with intense plasma viral loads lasting for over 40 days (22). Thus, this mouse model may be valuable for the study of HIV-1 infection. However, a serious problem remains. The mice showed symptoms of a wasting condition and a hunched back 5 to 7 months after HSC transplantation, following which most of them died. This life span is not sufficient if we are to better understand HIV pathogenesis and to develop novel anti-HIV countermeasures, because more than 4 months posttransplantation is required for the development of human T cells before HIV-1 can be studied in mice.

In past studies for the construction of humanized mouse models using NOD/SCID, β2 microglobulin-deficient NOD/SCID (NOD/SCID/B2m^{null}) or NOG mice, the mice were subjected to total body irradiation or given drugs for HSC transplantation (6, 9, 11, 14, 21, 23). Since NOG mice do not develop any thymic lymphomas in contrast to NOD/SCID or NOD/SCID/B2m^{null} mice (3, 19), the irradiation might influence the reduction of their life spans. In this study, we therefore searched for optimal conditions for HSC transplantation and consequently found that in NOG mice, myeloablation procedures were not required for human cell generation. Importantly, these mice stably survived

* Corresponding author. Mailing address for Naoki Yamamoto: AIDS Research Center, National Institute of Infectious Diseases, 1-23-1 Toyama, Shinjuku-ku, Tokyo 162-8640, Japan. Phone: 81-3-5285-1111. Fax: 81-3-5285-1165. E-mail: nyama@nih.go.jp. Mailing address for Norio Shimizu: Department of Virology, Division of Medical Science, Medical Research Institute, Tokyo Medical and Dental University, 1-5-45 Yushima, Bunkyo-ku, Tokyo 113-8519, Japan. Phone and fax: 81-3-5803-5811. E-mail: nshivir@tmd.ac.jp.

▽ Published ahead of print on 19 September 2007.

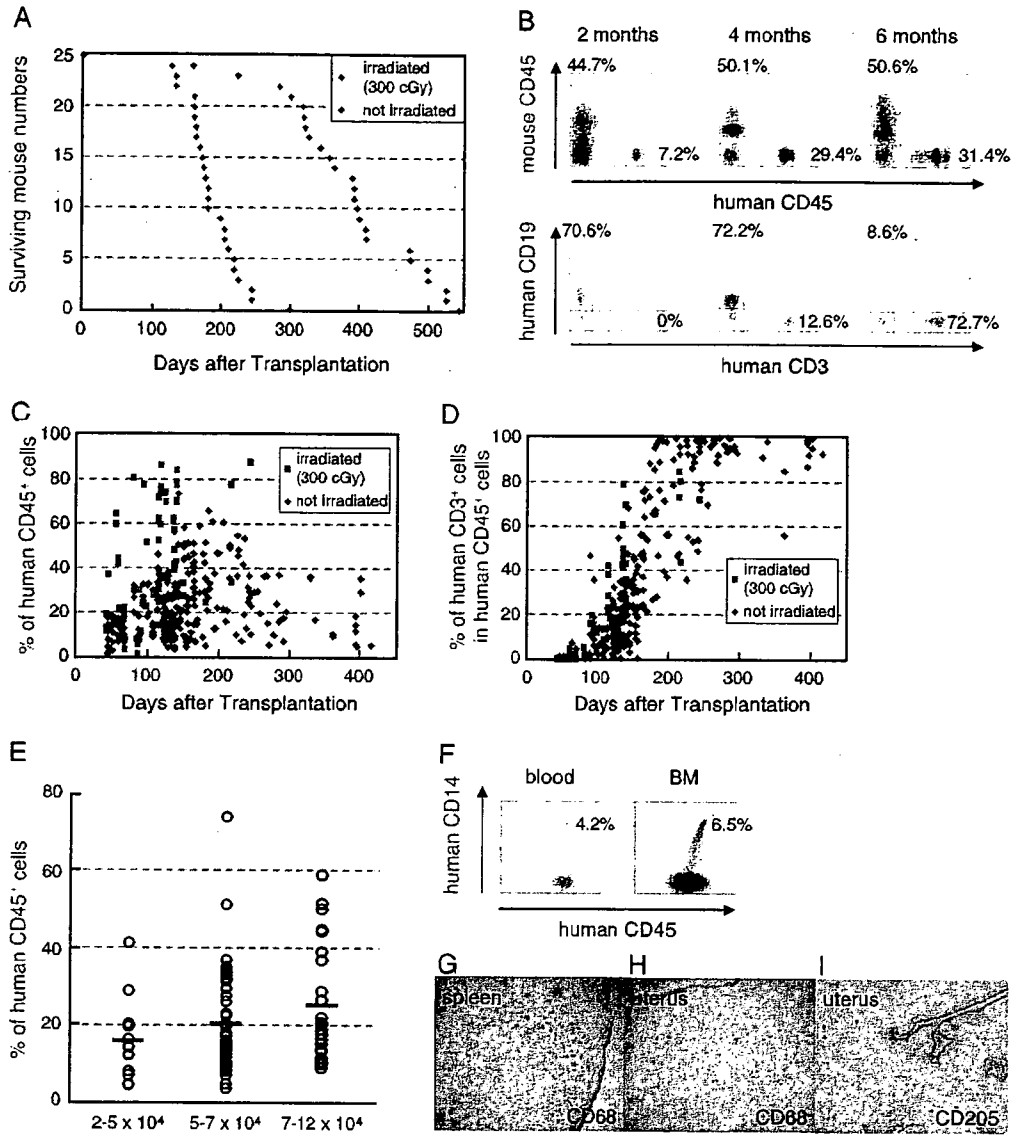

FIG. 1. Human cell generation in hematopoietic stem cell-engrafted hNOG mice with or without myeloablation. (A) Life spans of NOG mice transplanted with human stem cells after receiving 300 cGy irradiation (n = 25) or not receiving irradiation (n = 25). (B) Representative flow cytometric profiles of the mice from 2 to 6 months after transplantation without irradiation. The ratio of human to murine $CD45^+$ cells and that of human $CD3^+$ cells to $CD19^+$ cells are shown. Note that the mice generated human $CD45^+$ leukocytes that eventually developed human $CD19^+$ B cells first and then $CD3^+$ T cells. (C and D) Percentages of human $CD45^+$ cells (C) and $CD3^+$ T cells in human $CD45^+$ cells (D) in peripheral blood from 65 mice that received 300 cGy irradiation and 222 nonirradiated mice 40 to 413 days after transplantation. (E) Summary of engraftment levels in nonirradiated mice transplanted with 2×10^4 to 5×10^4 cells (n = 11), 5×10^4 to 7×10^4 cells (n = 53), or 7×10^4 to 12×10^4 (n = 30) human stem cells. Percentages of human $CD45^+$ leukocytes in peripheral blood during 4 to 5 months after transplantation were shown. The horizontal black bars indicate the averages of the groups. (F to I) Flow cytometric analysis and immunohistochemical analysis of the expression of myelomonocytic markers in nonirradiated mice 4 months after transplantation. Human $CD14^+$ monocytes/macrophages were recognized in peripheral blood and BM (F). A gate was set on the human $CD45^+$ population. Human $CD68^+$ macrophages and $CD205^+$ DCs were also detected in spleen (G) and uterus (H and I). Visualization was performed with 5-bromo-4-chloro-3-indolylphosphate (BCIP). The original magnifications were ×100 (G and H) and ×200 (I).

longer than 300 days after the HSC transplantation, which allowed further investigation of HIV-1 pathogenesis and progression to disease state in the animals.

NOG mice constructed with HSCs without myeloablation showed prolonged survival time and stable human cell generation. Six- to eight-week-old female NOG mice were obtained from the Central Institute for Experimental Animals (Kawasaki, Japan), and human cord blood-derived $CD34^+$ HSCs (2×10^4 to 12×10^4 cells) were injected intravenously with or without irradiation. As shown in Fig. 1A, most of the mice that received 300 cGy irradiation were dead within 250 days post-transplantation (mean survival time, 188 days). In contrast, more than 80% of the mice with transplanted HSCs without irradiation survived over 300 days (mean survival time, 387

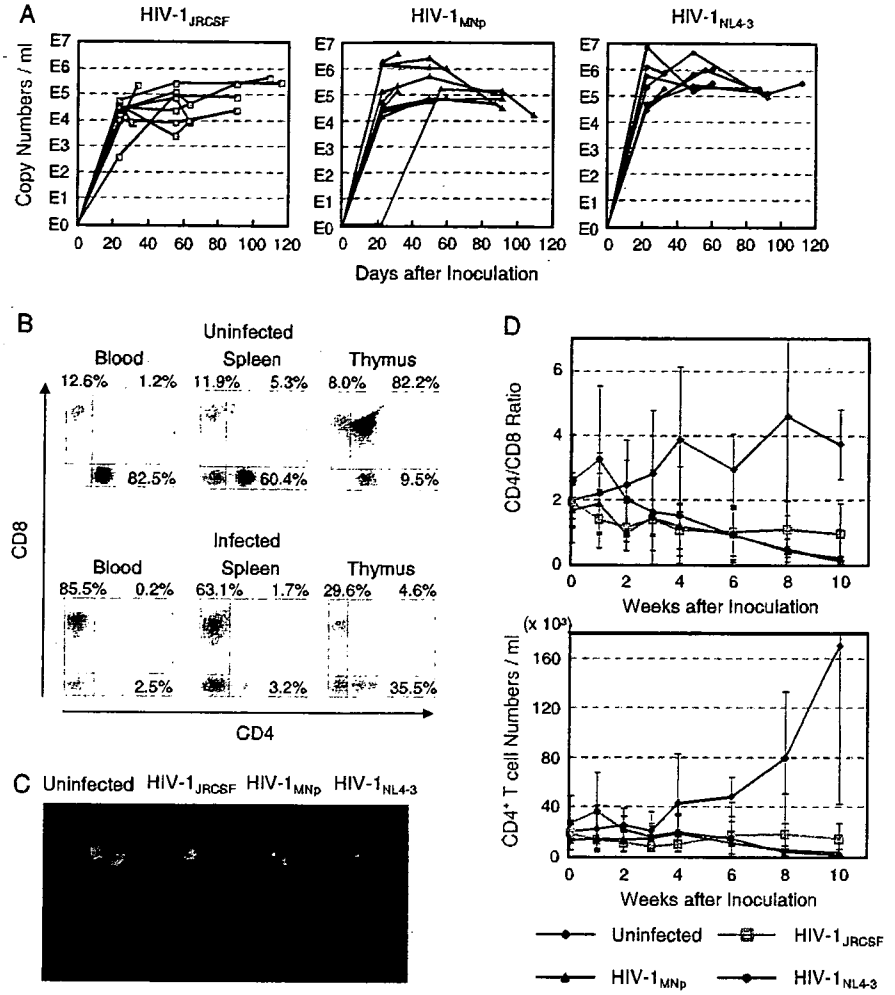

FIG. 2. Long-lasting viremia and $CD4^+$ T-cell depletion in R5- and X4-tropic HIV-1-infected hNOG mice. (A) Viral copy numbers in plasma from 29 mice intravenously inoculated with R5-tropic HIV-1_{JRCSF} (65,000 $TCID_{50}$; $n = 11$), X4-tropic HIV-1_{MNp} (20,000 $TCID_{50}$; $n = 10$), and X4-tropic HIV-1_{NL4-3} (60,000 $TCID_{50}$; $n = 8$). RNA viral copy numbers were measured using a real-time PCR quantification assay as previously described (22). (B) The percentages of $CD4^-$ $CD8^+$ (top left), $CD4^+$ $CD8^+$ (top right), and $CD4^+$ $CD8^-$ (bottom right) cells in blood, spleen, and thymus from a uninfected control mouse and a V-1_{NL4-3}-infected mouse (32 days postinfection). These two mice were constructed with HSCs from the same cord blood donor, and sacrificed 181 and 169 days after transplantation, respectively. A gate was set on the human $CD45^+$ population. (C) Comparison of the apparent size of mesenteric LN from uninfected mice or mice infected with HIV-1_{JRCSF} (109 days postinfection), HIV-1_{MNp} (109 days postinfection), or HIV-1_{NL4-3} (112 days postinfection). A uninfected control mouse was sacrificed 249 days after transplantation, and three HIV-1-infected mice were sacrificed 246, 246, and 249 days after transplantation. (D) Comparison of CD4/CD8 T-cell ratios and absolute $CD4^+$ T-cell numbers in peripheral blood from uninfected control mice ($n = 7$), R5-tropic HIV-1_{JRCSF}-infected mice ($n = 7$), X4-tropic HIV-1_{MNp}-infected mice ($n = 5$), and X4-tropic HIV-1_{NL4-3}-infected mice ($n = 6$). Results are expressed as means ± standard deviations (error bars).

days). These mice were successfully engrafted with HSCs, resulting first in the generation of human $CD19^+$ B cells and subsequently in the generation of human $CD3^+$ T cells (Fig. 1B). Figure 1C and D show the percentages of human $CD45^+$ leukocytes and human $CD3^+$ T cells in peripheral blood at 40 to 413 days after HSC transplantation. Up to 74% of leukocytes in peripheral blood samples were reconstituted with human cells in nonirradiated mice (mean ± standard deviation, 22.8% ± 14.0%; $n = 222$), and this was maintained over 400 days after transplantation (Fig. 1C). Although higher levels of human cell reconstitution were observed in the irradiated mice (45.2% ± 23.9%; $n = 65$) (Fig. 1C), which may be due to reduction of absolute numbers of murine cells by destruction of their progenitor cells in bone marrow (BM), human $CD3^+$ T cells developed with similar kinetics between the two groups (Fig. 1D). Figure 1E shows the engraftment efficiency of NOG mice transplanted with different numbers of HSCs without irradiation. More than 2×10^4 HSCs could be stably engrafted, and the levels of human cell reconstitution increased relative to the number of transplanted cells.

We further analyzed the development of human monocytes, macrophages, and DCs in the mice with transplanted HSCs without irradiation. Human $CD14^+$ monocytes were detected in peripheral blood and BM using flow cytometry (Fig. 1F), and many human $CD68^+$ macrophages were observed in various organs, including spleen (Fig. 1G), uterus (Fig. 1H), ovary, and lung (data not shown). Human $CD205^+$ DCs were also detected in spleen (data not shown) and uterus (Fig. 1I). These

TABLE 1. CD4/CD8 ratios in peripheral blood and spleen and $CD4^+$ $CD8^+$ cells in thymus of groups of uninfected and HIV-1-infected mice[a]

Group and mouse identification no.	No. of days after inoculation	CD4/CD8 ratio		% of $CD4^+$ $CD8^+$ cells in thymus	No. of RNA viral copies/ml
		Blood	Spleen		
Uninfected control group (n = 15)		2.92 ± 1.68	2.78 ± 1.46	67.8 ± 20.5	
$HIV\text{-}1_{JRCSF}$-infected group					
1	30	1.86	0.88	77.1	9,078
2	30	0.46	0.53	12.5	7,703
3	33	2.61	2.17	85.7	223,020
4	63	0.17	0.27	25.5	9,965
5	63	0.36	0.44	27.2	8,734
6	63	0.18	0.88	69.6	42,198
7	90	0.03	0.37	82.5	24,441
8	90	0.30	0.79	84.6	24,454
9	90	1.77	1.55	56.9	80,636
10	109	0.20	0.17	43.4	470,392
11	116	0.09	0.78	11.8	299,080
$HIV\text{-}1_{MNp}$-infected group					
1	31	0.82	0.44	34.6	3,709,520
2	31	1.02	0.61	90.2	219,971
3	31	1.64	1.57	78.2	135,592
4	59	0.21	0.38	35.4	78,848
5	59	0.10	0.07	77.0	1,039,716
6	87	0.20	0.40	0.5	49,080
7	87	0.19	0.08	11.7	121,817
8	91	0.04	0.04	82.9	30,706
9	91	0.28	0.10	1.2	7,407
10	109	0.00	0.21	2.8	17,310
$HIV\text{-}1_{NL4\text{-}3}$-infected group					
1	32	1.01	0.81	64.5	195,375
2	32	0.03	0.05	4.6	770,721
3	60	0.21	0.13	3.9	1,108,003
4	60	0.14	ND[b]	ND	328,375
5	87	0.03	0.04	1.0	201,207
6	92	0.03	0.17	11.1	90,831
7	92	0.03	0.03	1.4	135,514
8	112	0.30	0.23	0.2	325,202

[a] Twenty-nine mice inoculated with R5-tropic $HIV\text{-}1_{JRCSF}$ (n = 11), X4-tropic $HIV\text{-}1_{MNp}$ (n = 10), or X4-tropic $HIV\text{-}1_{NL4\text{-}3}$ (n = 8) were sacrificed 161 to 249 days after HSC transplantation. Fifteen uninfected control mice were sacrificed 174 to 249 days after transplantation, and results for the control group are expressed as means ± standard deviations.

[b] ND, not determined because of a lack of cells.

observations were similar to those seen in irradiated mice as shown in our previous report (22). Thus, humanized NOG (hNOG) mice without any myeloablation procedures allowed sufficient development of human cells to study HIV-1 pathogenesis.

hNOG mice induced systemic and long-lasting HIV-1 infection with $CD4^+$ T-cell depletion. We prepared 29 stem cell-transplanted hNOG mice and inoculated them intravenously with a high dose of R5-tropic $HIV\text{-}1_{JRCSF}$ (65,000 50% tissue culture infective doses [$TCID_{50}$]), X4-tropic $HIV\text{-}1_{MNp}$ (20,000 $TCID_{50}$), or X4-tropic $HIV\text{-}1_{NL4\text{-}3}$ (60,000 $TCID_{50}$) at 122 to 150 days posttransplantation. Then, plasma viral RNA copy numbers were measured at successive time points. The mice showed marked, long-lasting viremia state for more than 3 months, reaching the highest levels of 3.0×10^5 copies/ml from $HIV\text{-}1_{JRCSF}$-infected mice, 3.7×10^6 copies/ml from $HIV\text{-}1_{MNp}$-infected mice, and 7.8×10^6 copies/ml from $HIV\text{-}1_{NL4\text{-}3}$-infected mice (Fig. 2A). None of the mice weakened or died as a result of HIV-1 infection throughout the entire follow-up period.

All the mice were sacrificed within 4 months postinfection, and the percentages of $CD4^+$ and $CD8^+$ cells in lymphoid tissues were analyzed by flow cytometry. In a representative HIV-1-infected mouse, as shown in Fig. 2B, CD4/CD8 ratios in blood and spleen significantly decreased with apparent loss of $CD4^+$ $CD8^+$ double positive thymocytes. The size of lymphoid tissues, such as thymus and lymph node (LN), in the HIV-1-infected mice was very small compared with uninfected mice (Fig. 2C), suggesting that they shrank as a result of HIV-1 infection. Table 1 illustrates the overall profile of CD4/CD8 ratios in blood and spleen and the percentages of $CD4^+$ $CD8^+$ thymocytes from the 29 HIV-1-infected mice. Most of the mice, both R5- and X4-tropic and HIV-1 infected, had reduced CD4/CD8 ratios in blood and spleen compared with unin-

TABLE 2. Comparison of DNA proviral copies in various organs from HIV-1-infected mice[a]

Organ	No. of HIV-1 DNA copies/100 ng DNA in mice infected with[b]:		
	HIV-1_{JRCSF}	HIV-1_{MNp}	HIV-1_{NL4-3}
Peripheral blood	60	6	UD
Spleen	793	1,143	2,115
Bone marrow	2,432	656	584
Thymus	23	2,074	17,374
Lymph node	2,103	942	2,115
Lung	239	145	177
Liver	74	49	12
Small intestine	ND	6	9
Ovary	24	122	10
Uterus	14	5	16
Rectum	UD	16	11
Heart	9	UD	UD
Skin	UD	UD	138
Brain	UD	2	UD
Eyeball	3	25	UD

[a] Viral DNA was extracted from various organs of mice infected with HIV-1_{JRCSF} (33 days postinfection), HIV-1_{MNp} (59 days postinfection), and HIV-1_{NL4-3} (60 days postinfection). Determination of HIV-1 DNA copy numbers was performed by real-time PCR assay as previously described (22).
[b] UD, undetected; ND, not done.

fected control mice. On the other hand, a reduction of $CD4^+$ $CD8^+$ thymocytes was observed especially in X4-tropic HIV-1-infected mice, which seemed to correlate with the predominant expression of CXCR4 on the thymocytes as we previously described (22). Interestingly, two mice that were infected with HIV-1_{MNp} (mouse identification number 5 and 8) maintained their high percentages of $CD4^+$ $CD8^+$ thymocytes in spite of significant CD4/CD8 decline in their blood and spleen, suggesting no direct relationship between thymic T-cell depletion and CD4/CD8 decrease in peripheral blood or spleen by HIV-1 infection.

In one mouse from each R5- and X4-tropic HIV-infected group, HIV-1 proviral DNA copy numbers in various organs were measured by real-time PCR assay (Table 2). High HIV DNA copy numbers were detected in the spleen, BM, and LN of the R5-tropic HIV-1-infected mouse and in the thymus, spleen, and LN of the X4-tropic HIV-1-infected mice. In addition, HIV DNA copies were detectable in various other organs, including the lung, liver, ovary, and uterus. The fact that many human $CD68^+$ macrophages, the source of HIV-1 throughout the body (7, 8), were recognized in these organs (22) (Fig. 1H) may help explain the susceptibility of these organs to HIV-1.

To further investigate the progression of $CD4^+$ T-cell depletion by HIV-1 infection, 25 mice 120 to 151 days after HSC transplantation were randomly separated into groups of uninfected control mice (n = 7), HIV-1_{JRCSF}-inoculated mice (n = 7), HIV-1_{MNp}-inoculated mice (n = 5), and HIV-1_{NL4-3}-inoculated mice (n = 6), and then CD4/CD8 ratios and absolute $CD4^+$ T-cell numbers in peripheral blood were monitored at regular intervals. X4-tropic HIV-infected mice showed gradual decreases of their CD4/CD8 ratios and $CD4^+$ T-cell numbers, which eventually resulted in an almost complete depletion from peripheral blood (Fig. 2D). While $CD4^+$ T-cell depletion was also seen in R5-tropic HIV-infected mice, this was less prominent compared with X4-tropic HIV-1-infected mice (Fig. 2D). This pattern of R5- versus X4-tropic HIV-1 infection seems to correlate with the general observation that the emergence of X4-tropic HIVs accelerates $CD4^+$ T-cell decline and disease progression in HIV patients (12, 20).

In this study, we successfully prolonged the life span of hNOG mice by improving the HSC transplantation method and further clarified characteristics of HIV-1 infection in the mice including the following: (i) high levels of viremia lasting over 3 months, (ii) $CD4^+$ T-cell depletion in peripheral blood and spleen regardless of thymic T-cell loss, (iii) systemic HIV-1 infection not only in lymphoid tissues but also in various other organs, and (iv) a different rate of $CD4^+$ T-cell depletion for R5- versus X4-tropic HIV-1 strains. Recently, several studies on HIV-1 infection in $Rag2^{-/-}$ $\gamma c^{-/-}$ mice, transplanted with HSCs at birth, have also been reported (1, 2, 5, 24). The mice showed high susceptibility to both R5- and X4-tropic HIVs and long-term viremia with $CD4^+$ T-cell depletion, which is partly similar to our present results. However, the efficiency of human cell generation in $Rag2^{-/-}$ $\gamma c^{-/-}$ mice strongly depends on the dose of irradiation, and levels of chimerism in mice are not stable even receiving 550 to 750 cGy irradiation, which does eventually induces reduction of their life spans (5). In contrast, very stable engraftment of HSCs and subsequent human cell generation were noted in our hNOG mice even without any myeloablation procedures. Their long life spans and long-term human cell reconstitution allowed persistent HIV-1 infections mirroring HIV-1 infections in humans. Thus, this hNOG mouse system is a very useful tool as an advanced mouse model for the study of AIDS progression and long-term evaluation of new anti-HIV-1 drugs.

We thank Tomohiro Morio, Ken Watanabe, and Eiko Ogata of Tokyo Medical and Dental University for their helpful comments and skillful technical support. We are also grateful to Yukari Sasaki and Kazuhiro Takimoto of the National Institute of Infectious Diseases and Teruaki Tanaka and Junichi Fujita of the Nihon University School of Medicine for their management of animals. Human umbilical cord blood samples were obtained from the Tokyo Cord Blood Bank of the Nihon University School of Medicine.

This work was supported by a grant from the Ministry of Education, Culture, Sports, Science, and Technology to promote open research for young academics and specialists.

REFERENCES

1. Baenziger, S., R. Tussiwand, E. Schlaepfer, L. Mazzucchelli, M. Heikenwalder, M. O. Kurrer, S. Behnke, J. Frey, A. Oxenius, H. Joller, A. Aguzzi, M. G. Manz, and R. F. Speck. 2006. Disseminated and sustained HIV infection in $CD34^+$ cord blood cell-transplanted $Rag2^{-/-}$ $\gamma c^{-/-}$ mice. Proc. Natl. Acad. Sci. USA 103:15951–15956.
2. Berges, B. K., W. H. Wheat, B. E. Palmer, E. Connick, and R. Akkina. 2006. HIV-1 infection and CD4 T cell depletion in the humanized $Rag2^{-/-}$ $\gamma c^{-/-}$ (RAG-hu) mouse model. Retrovirology 3:76.
3. Christianson, S. W., D. L. Greiner, R. A. Hesselton, J. H. Leif, E. J. Wagar, I. B. Schweitzer, T. V. Rajan, B. Gott, D. C. Roopenian, and L. D. Shultz. 1997. Enhanced human $CD4^+$ T cell engraftment in beta2-microglobulin-deficient NOD-scid mice. J. Immunol. 158:3578–3586.
4. Fais, S., C. Lapenta, S. M. Santini, M. Spada, S. Parlato, M. Logozzi, P. Rizza, and F. Belardelli. 1999. Human immunodeficiency virus type 1 strains R5 and X4 induce different pathogenic effects in hu-PBL-SCID mice, depending on the state of activation/differentiation of human target cells at the time of primary infection. J. Virol. 73:6453–6459.
5. Gorantla, S., H. Sneller, L. Walters, J. G. Sharp, S. J. Pirruccello, J. T. West, C. Wood, S. Dewhurst, H. E. Gendelman, and L. Poluektova. 2007. Human immunodeficiency virus type 1 pathobiology studied in humanized BALB/c-$Rag2^{-/-}\gamma_c^{-/-}$ mice. J. Virol. 81:2700–2712.
6. Hiramatsu, H., R. Nishikomori, T. Heike, M. Ito, K. Kobayashi, K. Katamura, and T. Nakahata. 2003. Complete reconstitution of human lym-

phocytes from cord blood CD34$^+$ cells using the NOD/SCID/γ_c^{null} mice model. Blood 102:873–880.
7. Igarashi, T., C. R. Brown, Y. Endo, A. Buckler-White, R. Plishka, N. Bischofberger, V. Hirsch, and M. A. Martin. 2001. Macrophage are the principal reservoir and sustain high virus loads in rhesus macaques after the depletion of CD4$^+$ T cells by a highly pathogenic simian immunodeficiency virus/HIV type 1 chimera (SHIV): implications for HIV-1 infections of humans. Proc. Natl. Acad. Sci. USA 98:658–663.
8. Igarashi, T., O. K. Donau, H. Imamichi, M. J. Dumaurier, R. Sadjadpour, R. J. Plishka, A. Buckler-White, C. Buckler, A. F. Suffredini, H. C. Lane, J. P. Moore, and M. A. Martin. 2003. Macrophage-tropic simian/human immunodeficiency virus chimeras use CXCR4, not CCR5, for infections of rhesus macaque peripheral blood mononuclear cells and alveolar macrophages. J. Virol. 77:13042–13052.
9. Ito, M., H. Hiramatsu, K. Kobayashi, K. Suzue, M. Kawahata, K. Hioki, Y. Ueyama, Y. Koyanagi, K. Sugamura, K. Tsuji, T. Heike, and T. Nakahata. 2002. NOD/SCID/γ_c^{null} mouse: an excellent recipient mouse model for engraftment of human cells. Blood 100:3175–3182.
10. Kaneshima, H., L. Su, M. L. Bonyhadi, R. I. Connor, D. D. Ho, and J. M. McCune. 1994. Rapid-high, syncytium-inducing isolates of human immunodeficiency virus type 1 induce cytopathicity in the human thymus of the SCID-hu mouse. J. Virol. 68:8188–8192.
11. Kollet, O., A. Peled, T. Byk, H. Ben-Hur, D. Greiner, L. Shultz, and T. Lapidot. 2000. β2 Microglobulin-deficient (B2m^{null}) NOD/SCID mice are excellent recipients for studying human stem cell function. Blood 95:3102–3105.
12. Koot, M., I. P. Keet, A. H. Vos, R. E. de Goede, M. T. Roos, R. A. Coutinho, F. Miedema, P. T. Schellekens, and M. Tersmette. 1993. Prognostic value of HIV-1 syncytium-inducing phenotype for rate of CD4$^+$ cell depletion and progression to AIDS. Ann. Intern. Med. 118:681–688.
13. Koyanagi, Y., Y. Tanaka, J. Kira, M. Ito, K. Hioki, N. Misawa, Y. Kawano, K. Yamasaki, R. Tanaka, Y. Suzuki, Y. Ueyama, E. Terada, T. Tanaka, M. Miyasaka, T. Kobayashi, Y. Kumazawa, and N. Yamamoto. 1997. Primary human immunodeficiency virus type 1 viremia and central nervous system invasion in a novel hu-PBL-immunodeficient mouse strain. J. Virol. 71:2417–2424.
14. Matsumura, T., Y. Kametani, K. Ando, Y. Hirano, I. Katano, R. Ito, M. Shiina, H. Tsukamoto, Y. Saito, Y. Tokuda, S. Kato, M. Ito, K. Motoyoshi, and S. Habu. 2003. Functional CD5$^+$ B cells develop predominantly in the spleen of NOD/SCID/γc^{null} (NOG) mice transplanted either with human umbilical cord blood, bone marrow, or mobilized peripheral blood CD34$^+$ cells. Exp. Hematol. 31:789–797.
15. McCune, J., H. Kaneshima, J. Krowka, R. Namikawa, H. Outzen, B. Peault, L. Rabin, C. C. Shih, E. Yee, M. Lieberman, I. Weissman, and L. Shultz. 1991. The SCID-hu mouse: a small animal model for HIV infection and pathogenesis. Annu. Rev. Immunol. 9:399–429.
16. Mosier, D. E., R. J. Gulizia, S. M. Baird, D. B. Wilson, D. H. Spector, and S. A. Spector. 1991. Human immunodeficiency virus infection of human-PBL-SCID mice. Science 251:791–794.
17. Mosier, D. E., R. J. Gulizia, P. D. MacIsaac, B. E. Torbett, and J. A. Levy. 1993. Rapid loss of CD4$^+$ T cells in human-PBL-SCID mice by noncytopathic HIV isolates. Science 260:689–692.
18. Namikawa, R., H. Kaneshima, M. Lieberman, I. L. Weissman, and J. M. McCune. 1988. Infection of the SCID-hu mouse by HIV-1. Science 242:1684–1686.
19. Shultz, L. D., P. A. Schweitzer, S. W. Christianson, B. Gott, I. B. Schweitzer, B. Tennent, S. McKenna, L. Mobraaten, T. V. Rajan, D. L. Greiner, et al. 1995. Multiple defects in innate and adaptive immunologic function in NOD/LtSz-scid mice. J. Immunol. 154:180–191.
20. Tersmette, M., R. A. Gruters, F. de Wolf, R. E. de Goede, J. M. Lange, P. T. Schellekens, J. Goudsmit, H. G. Huisman, and F. Miedema. 1989. Evidence for a role of virulent human immunodeficiency virus (HIV) variants in the pathogenesis of acquired immunodeficiency syndrome: studies on sequential HIV isolates. J. Virol. 63:2118–2125.
21. Ueda, T., H. Yoshino, K. Kobayashi, M. Kawahata, Y. Ebihara, M. Ito, S. Asano, T. Nakahata, and K. Tsuji. 2000. Hematopoietic repopulating ability of cord blood CD34$^+$ cells in NOD/Shi-*scid* mice. Stem Cells 18:204–213.
22. Watanabe, S., K. Terashima, S. Ohta, S. Horibata, M. Yajima, Y. Shiozawa, M. Z. Dewan, Z. Yu, M. Ito, T. Morio, N. Shimizu, M. Honda, and N. Yamamoto. 2007. Hematopoietic stem cell-engrafted NOD/SCID/IL2Rγ^{null} mice develop human lymphoid systems and induce long-lasting HIV-1 infection with specific humoral immune responses. Blood 109:212–218.
23. Yahata, T., K. Ando, Y. Nakamura, Y. Ueyama, K. Shimamura, N. Tamaoki, S. Kato, and T. Hotta. 2002. Functional human T lymphocyte development from cord blood CD34$^+$ cells in nonobese diabetic/Shi-*scid*, IL-2 receptor γ null mice. J. Immunol. 169:204–209.
24. Zhang, L., G. I. Kovalev, and L. Su. 2007. HIV-1 infection and pathogenesis in a novel humanized mouse model. Blood 109:2978–2981.

Hematopoietic stem cell–engrafted NOD/SCID/IL2Rγ^{null} mice develop human lymphoid systems and induce long-lasting HIV-1 infection with specific humoral immune responses

Satoru Watanabe,[1] Kazuo Terashima,[2] Shinrai Ohta,[3] Shigeo Horibata,[3] Misako Yajima,[4] Yoko Shiozawa,[1] M. Zahidunnabi Dewan,[2,3] Zhong Yu,[2] Mamoru Ito,[5] Tomohiro Morio,[6] Norio Shimizu,[1] Mitsuo Honda,[3] and Naoki Yamamoto[2,3]

[1]Department of Virology, Division of Medical Science, Medical Research Institute, Tokyo Medical and Dental University, Japan; [2]Department of Molecular Virology, Graduate School of Medicine, Tokyo Medical and Dental University, Japan; [3]AIDS Research Center, National Institute of Infectious Diseases, Tokyo, Japan; [4]Department of Infectious Diseases, National Research Institute for Child Health and Development, Tokyo, Japan; [5]Central Institute for Experimental Animals, Kanagawa, Japan; and [6]Department of Pediatrics and Developmental Biology, Graduate School of Medicine, Tokyo Medical and Dental University, Japan

Critical to the development of an effective HIV/AIDS model is the production of an animal model that reproduces long-lasting active replication of HIV-1 followed by elicitation of virus-specific immune responses. In this study, we constructed humanized nonobese diabetic/severe combined immunodeficiency (NOD/SCID)/interleukin-2 receptor γ-chain knockout (IL2Rγ^{null}) (hNOG) mice by transplanting human cord blood–derived hematopoietic stem cells that eventually developed into human B cells, T cells, and other monocytes/macrophages and dendritic cells associated with the generation of lymphoid follicle–like structures in lymphoid tissues. Expressions of CXCR4 and CCR5 antigens were recognized on CD4$^+$ cells in peripheral blood, the spleen, and bone marrow, while CCR5 was not detected on thymic CD4$^+$ T cells. The hNOG mice showed marked, long-lasting viremia after infection with both CCR5- and CXCR4-tropic HIV-1 isolates for more than the 40 days examined, with R5 virus–infected animals showing high levels of HIV-DNA copies in the spleen and bone marrow, and X4 virus–infected animals showing high levels of HIV-DNA copies in the thymus and spleen. Furthermore, we detected both anti–HIV-1 Env gp120– and Gag p24–specific antibodies in animals showing a high rate of viral infection. Thus, the hNOG mice mirror human systemic HIV infection by developing specific antibodies, suggesting that they may have potential as an HIV/AIDS animal model for the study of HIV pathogenesis and immune responses. (Blood. 2007; 109:212-218)

Introduction

Current animal models for either human immunodeficiency virus type 1 (HIV-1) or simian immunodeficiency virus (SIV) suffer from the lack of a system precisely mirroring human HIV infection and the progression to disease state.[1] In current animal models with HIV infection, such as chimpanzees, animals do not develop AIDS.[1] Past animal models for HIV infection have relied on humanized severe combined immunodeficiency (hSCID) mice models to study prospective anti-HIV drugs and vaccines. SCID-hu (Thy/Liv) mice, engrafted with human fetal thymus and liver tissue in the renal subcapsular region, were first reported as the small-animal model.[2] Because human T cells are generated within the engrafted thymus, this model has been used for the study of thymopoiesis[3-6] and hematopoiesis[7,8] under the burden of HIV-1 infection. However, this model allows for a limited systemic HIV-1 infection, which is restricted mainly to the engrafted thymus. Another HIV mouse model, hu-PBL–SCID mice engrafted with human peripheral blood mononuclear cells (PBMCs),[9] has been actively used as a tool in developing antiretroviral therapy.[9-11] However, the infection persists for only a short time in association with rapid loss of CD4$^+$ T cells because there is no active hematopoiesis or thymopoiesis.[9,12,13] Furthermore, these mouse models fail to mirror certain key aspects of the human immune response, lacking normal lymphoid tissue and functional human antigen-presenting cells such as dendritic cells (DCs).[14] Thus, although these mouse models are valuable as animal models for HIV infection, the development of a mouse model more analogous to human HIV infection is needed if we are to better understand HIV pathogenesis and develop successful anti-HIV therapies and preventive vaccines.

To solve the difficult issue about the development of an ideal HIV mouse model, we initially selected a humanized nonobese diabetic (NOD)/SCID interleukin-2 receptor (IL-2R) γ-chain knockout (NOG) mouse[15] as a model animal because it has been suggested that multilineage cells, including human T, B, and natural killer (NK) cells, differentiate in these mice when given transplants of human CD34$^+$ hematopoietic stem cells.[16-18] In the current study, we further reveal the kinetics of differentiation of human B and T cells, monocytes/macrophages, and DCs in the mice that received transplants, and we characterize the animals by infection with both CCR5 (R5)– and CXCR4 (X4)-tropic HIV strains. Since our hNOG mice show stable and systemic infection of both R5- and X4-tropic HIV for more than

Submitted April 20, 2006; accepted August 12, 2006. Prepublished online as *Blood* First Edition Paper, September 5, 2006; DOI 10.1182/blood-2006-04-017681.

The publication costs of this article were defrayed in part by page charge payment. Therefore, and solely to indicate this fact, this article is hereby marked "advertisement" in accordance with 18 USC section 1734.

the 40 days studied, and HIV-specific antibodies are detectable in the animals with high plasma viral loads and HIV-DNA copy numbers, we also discuss the suitability of HIV-hNOG mice as an animal model for HIV-1 infection.

Materials and methods

Transplantation of human CB-derived hematopoietic stem cells in NOG mice

Human cord blood (CB) was obtained from Saiseikai Central hospital (Minato-ku, Tokyo, Japan) and Tokyo Cord Blood Bank (Katsushika-ku, Tokyo, Japan) after obtaining informed consent. All research on human subjects was approved by the Institutional Review Board of each institution participating in the project. CB mononuclear cells were separated by Ficoll-Hypaque density gradient. $CD34^+$ hematopoietic stem cells were isolated using a magnetic-activated cell sorting (MACS) Direct CD34 Progenitor Cell Isolation Kit (Miltenyi Biotec, Bergisch Gladbach, Germany) according to the manufacturer's instructions. More than 95% of $CD34^+$ cells were positively selected after 2 time-enrichment manipulations. Cells were either immediately used for the transplantation or frozen until use. NOG mice were obtained from the Central Institute for Experimental Animals (Kawasaki, Japan) and maintained under specific pathogen-free (SPF) conditions in the animal facility of the National Institute of Infectious Diseases (NIID; Tokyo, Japan). Mice used in these studies were free of known pathogenic viruses, herpes viruses, bacteria, and parasites. They were housed in accordance with the Guidelines for Animal Experimentation of the Japanese Association for Laboratory Animal Science (1987) under the Japanese Law Concerning the Protection and Management of Animals, and were maintained in accordance with the guidelines set forth by the Institutional Animal Care and Use Committee of NIID, Japan. Once approved by the Institutional Committee for Biosafety Level 3 experiments, these studies were conducted at the Animal Center, NIID, Japan, in accordance with the requirements specifically stated in the laboratory biosafety manual of the World Health Organization. Female mice (6 to 10 weeks old) were irradiated (300 cGy) and 1×10^4 to 1.2×10^5 $CD34^+$ cells were intravenously injected within 12 hours.

Flow cytometry

The purity of CB-derived $CD34^+$ cells after separation was evaluated by double staining with FITC-conjugated anti–human CD45 (J.33) and PE-conjugated anti–human CD34 (Class III 581) (all from Beckman Coulter, Fullerton, CA). After transplantation (1-7 months), peripheral blood, spleens, bone marrow (BM), and thymi were collected for flow cytometric analysis following staining with the following monoclonal antibodies (mAbs): FITC-conjugated anti–human CD45 (J.33), CD3 (UCHT1), CD4 (13B8.2), CD19 (J4.119), CD45RO (UCHL1) (all from Beckman Coulter), and CCR5 (2D7; BD Pharmingen, San Diego, CA); PE-conjugated anti–human CD4 (13B8.2), CD8 (B9.11), CD19 (J4.119), CD45RA (ALB11) (all from Beckman Coulter), and CXCR4 (44717; R&D Systems, Minneapolis, MN); anti–mouse CD45 (YW62.3; Beckman Coulter); ECD-conjugated anti–human CD45 (J.33; Beckman Coulter); and PC5-conjugated anti–human CD8 (T8) and CD14 (Rm052) (all from Beckman Coulter). Flow cytometric analysis was conducted by 2- or 4-color staining using an EpicsXL (Beckman Coulter).

Immunohistochemistry

Organs were snap-frozen following embedding in OCT compound (Sakura Finetechnical, Tokyo, Japan). Frozen sections were air-dried and fixed in acetone. HIV-1–infected organs were fixed in 4% paraformaldehyde and embedded in OCT compound following immersion in gradient sucrose (5%-30%). Fixed samples were stained with the following mAbs: anti–human CD45 (1.22/4014; Nichirei, Tokyo, Japan), CD3 (UCHT1; DAKO, Glostrup, Denmark), CD20 (L26; DAKO), CD68 (KP1; DAKO), CD205 (MG38; eBioscience, San Diego, CA), and DRC-1 (R4/23; DAKO) for follicular dendritic cells (FDCs); anti–mouse FDC-M1 (BD Pharmingen) for murine FDCs; and HIV-1 Gag p24 (DAKO) for detection of infected cells. Biotin-labeled goat $F(ab')_2$ anti–mouse immunoglobulin (Ig; ICN Biomedicals, Aurora, OH)– or biotin-labeled mouse $F(ab')_2$ anti–rat IgG (Jackson ImmunoResearch Laboratories, West Grove, PA) was used as the secondary antibody. Samples were treated with alkaline phosphatase (AP) or horseradish peroxidase (HRP)–streptavidin conjugate (ZYMED Laboratories Inc, San Francisco, CA). BCIP/NBT, DAB, or AEC (all from DAKO) was used for the visualization. Photographs were taken by light microscopy (Leica DMRA; Leica Microsystems Wetzlar, Wetzlar, Germany) using Leica HC PLAN APO lenses (10×/0.40 NA PH1). Leica Q550 was used for image processing.

Measurement of human Igs in mice plasma

Plasma concentrations of human IgM, IgG, and IgA in NOG mice that received transplants of human stem cells were determined by conventional human Ig quantitation assay at BML Inc (Tokyo, Japan).

Cells and viruses

Human embryonic kidney 293T cells and monkey kidney COS7 cells were cultured in RPMI 1640 supplemented with 10% fetal bovine serum (FBS) and antibiotics. The 293T cells and COS7 cells were used for transfection of DNA plasmids containing $HIV\text{-}1_{JRCSF}$ and simian/human immunodeficiency virus (SHIV)–C2/1, respectively. The SHIV-C2/1 strain contains the *env* gene of pathogenic HIV-1 strain 89.6.[19] Cell-free supernatant was collected and stored at −80°C before use. A primary clinical isolate, $HIV\text{-}1_{MNp}$, was kindly provided by Dr J. Sullivan of the University of Massachusetts Medical School (Worcester, MA). PBMCs isolated from HIV-1–seronegative individuals were cultured in RPMI 1640 supplemented with 10% FBS and antibiotics with 5 μg of phytohemagglutinin (PHA)/mL for 3 or 7 days (PHA-PBMCs). $HIV\text{-}1_{MNp}$ was propagated in PHA-PBMCs, and cell-free virus stocks were stored at −80°C.

The 50% tissue-culture infectious dose ($TCID_{50}$) was determined using PHA-PBMCs and the endpoint dilution method. A 4-fold series of dilution was prepared from the virus stock, and then cells were mixed and cultured for 7 days for X4–HIV-1 and 14 days for R5–HIV-1 in RPMI 1640 supplemented with 20% FBS and antibiotics. The endpoints were determined by screening for the p24 antigen using Lumipulse (Fujirevio, Tokyo, Japan).

HIV-1 infection

All procedures for the infection and maintenance of NOG mice were performed in Biosafety Level 3 facilities at NIID under standard caging conditions. On days 102 to 132 after stem cell transplantation, 16 mice were inoculated intravenously with R5-tropic $HIV\text{-}1_{JRCSF}$ (65 000 $TCID_{50}$) or X4-tropic SHIV-C2/1 (50 000 $TCID_{50}$). On days 18 to 43 after inoculation, plasma was collected to determine HIV-RNA copy numbers, and spleen cells were prepared as single-cell suspensions to analyze the CD4/CD8 ratio using flow cytometry. A number (14) of other mice were inoculated intravenously with R5-tropic $HIV\text{-}1_{JRCSF}$ (200 or 65 000 $TCID_{50}$) or X4-tropic $HIV\text{-}1_{MNp}$ (180 or 20 000 $TCID_{50}$) on days 126 to 146 after transplantation. On days 18 to 40 after inoculation, plasma was collected for the determination of HIV-RNA copy numbers, and single-cell suspensions of the spleen, BM, and thymus were prepared for HIV-DNA measurement. The CD4/CD8 ratio in the spleen and percentages of human $CD45^+$ cells in organs were analyzed using flow cytometry.

Virologic analysis

Plasma viral RNA copy numbers were measured using a real-time quantification assay based on the TaqMan system (Applied Biosystems, Foster City, CA). Plasma viral RNA was extracted and purified using a QIAamp Viral RNA Mini Kit (Qiagen, Valencia, CA). The RNA was subjected to reverse transcription (RT) and amplification using a TaqMan One-Step RT–polymerase chain reaction (PCR) Master Mix Reagents Kit (PE Biosystems, Foster City, CA) with HIV-1 gag consensus primers

(forward, 5′-GGACATCAAGCAGCCATGCAA-3′; and reverse, 5′-TGCTATGTCACTTCCCCTTGG-3′) and an HIV-1 gag consensus TaqMan probe (FAM-5′-ACCATCAATGAGGAAGCTGCAGAA-3′-TAMRA). For SHIV-C2/1 analysis, primers (forward, 5′-AATGCAGAGCCCCAAGAAGAC-3′; and reverse, 5′-GGACCAAGGCCTAAAAAACCC-3′) and a TaqMan probe (FAM-5′-ACCATGTTATGGCCAAATGCCCAGAC-3′-TAMRA) were designed for targeting the SIVmac239 gag region.[20] Probed products were quantitatively monitored by their fluorescence intensity with the ABI7300 Real-Time PCR system (PE Biosystems). To obtain control RNA for quantification, HIV-1 gag RNA and SIVmac239 gag RNA were synthesized using T7 RNA polymerase and pKS460. Viral DNA was extracted and purified using a QIAamp DNA Mini Kit (Qiagen). Determination of HIV-1 DNA copy numbers was performed by real-time PCR assay with TaqMan Master mixture (PE Biosystems). Primers (forward, 5′-GGCTAACTAGGGAACCCACTG-3′; and reverse, 5′-CTGCTAGAGATTTTCCACACT-3′) and probes (FAM-5′-TAGTGTGTGCCCGTCTGTTGTGTGAC-3′-TAMRA) were designed for targeting the HIV-1 long terminal repeat region, R/U5. The viral DNA was quantified using LightCycler (Roche Diagnostics, Almere, The Netherlands). Viral RNA and DNA were calculated based on the standard curve of control RNA and DNA. All assays were carried out in duplicate.

HIV-antigen ELISA

Levels of anti–HIV-1 Igs against recombinant HIV-1_{IIIB} Env gp120, recombinant HIV-1_{MN} Env gp120, and recombinant HIV-1_{IIIB} Gag p24 (all from ImmunoDiagnostics Inc, Woburn, MA) in plasma from HIV-1–infected and –uninfected control mice were determined using a standard enzyme-linked immunosorbent assay (ELISA). Microplates (96-well) were coated overnight with 200 ng/well antigens, and plasma diluted 1:20, 1:60, and 1:180 with PBS were incubated for 1 hour. AP-labeled anti–human Igs (γ, α, and μ; Sigma-Aldrich, St Louis, MO) were used as secondary antibodies. P-nitrophenylphosphate (pNPP) Solution (WAKO Chemical USA, Richmond, VA) was used for the visualization. The enzyme reaction was stopped by addition of 0.1 M NaOH and read at 405 nm. All assays were carried out in triplicate.

Statistical analysis

Data were expressed as the mean value ± standard deviation (SD). Significant differences between data groups were determined by 2-sample Student *t* test analysis. A P value less than .05 was considered significant.

Results

Reconstitution of human lymphoid systems in hNOG mice

The initial studies describing the construction of humanized SCID mice used the human PBMC for infection of immunodeficiency viruses.[9,12,21] However, these hu-PBL-SCID mice showed a partial infection to the R5 virus and a relatively limited period of viral replication. To construct a more suitable mouse model mimicking HIV-1 infection in humans, we selected human CB stem cells as a transplant for NOG mice. NOG mice were inoculated intravenously with human CD34$^+$ hematopoietic stem cells, and their development of human lymphoid systems were then monitored. After transplantation (2 months), human CD45$^+$ leukocytes were recognized in both PB and the spleen, but most of the cells were human B cells (Figure 1A). Human T cells began to be recognized clearly in PB and the spleen 4 months after transplantation (Figure 1B) and gradually increased in level, as did human B cells (Figure 1C).

In Figure 1D, we summarized percentages of human CD3$^+$ T cells in human CD45$^+$ cells from 38 mice from 39 to 213 days after transplantation. Human CD3$^+$ T cells clearly increased 100 days after transplantation in both PB and the spleen. After transplantation (4 months), human CD3$^+$ T cells in the spleen preferably expressed CD45RA rather than CD45RO (70.8% ± 13.4% and 27.3% ± 38.8% in CD3$^+$ T cells, respectively; n = 5; Figure 1E), demonstrating that most of the T cells were in a naive state. In addition, plasma taken from 5 mice 113 to 143 days after transplantation showed that all mice produced human IgM, with concentrations ranging from 0.025 to 0.5 g/L, and that human IgG and IgA was also detected in some of the mice (ranges, 0.015-0.18 g/L and 0.003-0.012 g/L, respectively) (data not shown).

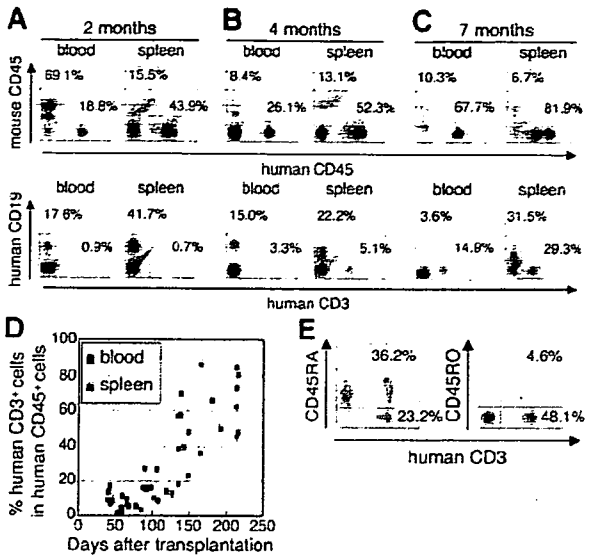

Figure 1. Flow cytometric analysis of human T cells in the peripheral blood and spleen in NOG mice given intravenous transplants of human CB-derived CD34$^+$ cells. (A-C) Representative profiles of the mice 2 months (A), 4 months (B), and 7 months (C) after transplantation. The ratio of human to murine CD45$^+$ cells and that of human CD3$^+$ to CD19$^+$ cells show an incremental increase in human CD45$^+$ cells and human CD3$^+$ cells from 2 to 7 months. (D) Change of net percentages of human CD3$^+$ T cells among human CD45$^+$ cells in peripheral blood and the spleen from 38 mice 39 to 213 days after transplantation. (E) CD45RA is more efficiently expressed than CD45RO on human CD3$^+$ T cells in spleen. A gate was set on the human CD45$^+$ population. The fluorescence-activated cell sorting (FACS) profile is representative of 1 in a group of 5 mice.

By 7 months after transplantation, human CD45$^+$ leukocytes comprised more than 80% to 90% of mononuclear cells in the spleen (Figure 1C), and most of the mice showed symptoms of a wasting condition and a hunched back. Based upon these results, we determined that the suitable period for HIV inoculation would be 4 to 5 months after transplantation.

Formation of lymphoid structures, including monocytes/macrophages, DCs, and FDCs

Next, using the hNOG mice at 4 months after transplantation, we investigated lymphoid structure formation and the development of human monocytes, macrophages, DCs, and FDCs, which are very important factors not only for elicitation of immune responses against foreign antigens, but also for the spread of HIV-1 infection in a body.[22-24] Human CD14$^+$ monocytes were detected in PB, the spleen, and BM using flow cytometry (Figure 2A). During immunohistochemical analysis, human CD45$^+$ leukocytes gathered in a form of follicle-like structures (FLSs) at the end of the central artery in the spleen (Figure 2B). From a serial section of the same region (Figure 2B-G), these structures consisted mainly of human CD20$^+$ B cells (Figure 2C) admixed with a small number of human CD3$^+$ T cells (Figure 2D). Hardly any human FDCs positive for DRC-1 were detected (data not shown), whereas a

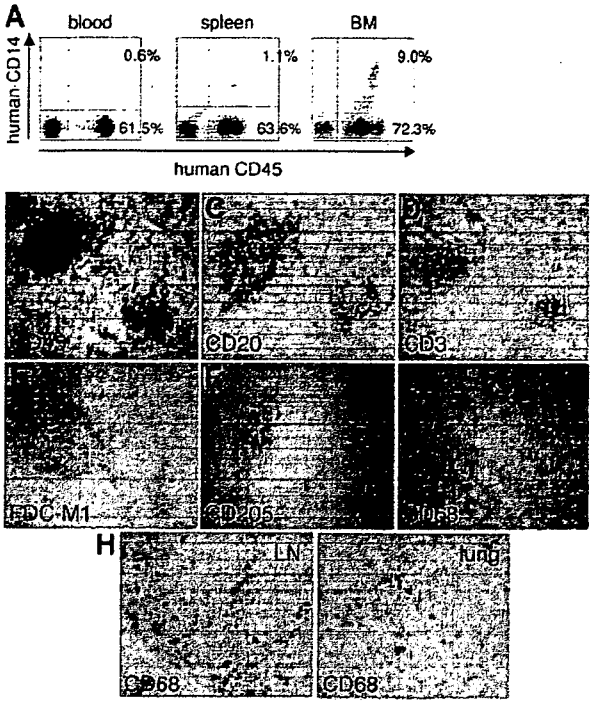

Figure 2. Flow cytometric analysis and immunohistochemical analysis of the expression of myelomonocytic markers in hNOG mice 4 months after transplantation. (A) Human CD14$^+$ monocytes/macrophages are recognized in peripheral blood, the spleen, and BM. (B-G) Immunohistochemical findings from serially sectioned spleen for the expressions of human CD45 (B), human CD20 (C), human CD3 (D), murine FDC (E), human CD205 (F), and human CD68 (G). (H) Human CD68$^+$ macrophages are also detected in the medulla of the LN and lung. Visualization was performed with BCIP (B-D, F-G), DAB (E), and AEC (H). Original magnification, ×100.

loose network of murine FDCs positive for FDC-M1 was recognized in the distal portion of the FLSs (Figure 2E). Human CD205$^+$ DCs were predominantly detected in a cluster form within the FLSs (Figure 2F), while human CD68$^+$ macrophages were scattered throughout the spleen (Figure 2G). Many human CD68$^+$ macrophages were also observed in various other organs, including the lymph nodes (LNs) and the lungs (Figure 2H).

Expression of HIV-1 coreceptors on CD4$^+$ cells in various tissues

Since the development of lymphoid tissues was recognized in hNOG mice, we focused on the expressions of HIV-1 coreceptors CXCR4 and CCR5 on human CD4$^+$ cells in these tissues. CXCR4 antigen was expressed in 36.5% ± 4.2% (n = 4) of the CD4$^+$ cells in PB (Figure 3A) and 78.1% ± 17.1% (n = 5) in the spleen (Figure 3B). CCR5$^+$ cells were detected in 15.5% ± 1.8% (n = 4) of CD4$^+$ cells in PB and 28.6% ± 12.6% (n = 5) in the spleen (Figure 3A-B). In the thymus, CD4$^+$CD8$^+$ thymocytes existed in 82.9% ± 4.4% (n = 5) as well as small numbers of CD4$^+$CD8$^-$ cells (6.4% ± 2.4%; n = 5) and CD4$^-$CD8$^+$ cells (7.7% ± 3.0%; n = 5), with the CXCR4 antigen expressed in 50.1% ± 4.5% (n = 5) of CD4$^+$ cells, while, as with normal human thymocytes,[25] CCR5$^+$ cells were almost undetectable, with less than 1% (0.6% ± 0.1%; n = 5) (Figure 3C). Human CD3$^+$ T cells and CD14$^+$ monocytes in BM were detected only in 3.2% ± 2.1% and 5.8% ± 3.8%, respectively, while CD4$^+$ cells were recognized in 18.1% ± 6.5%, with many expressing both CXCR4 (75.0% ± 23.1%) and CCR5 (81.3% ± 6.6%; n = 5; Figure 3D). Thus, distributions of HIV-1 coreceptor–positive cells in these lymphoid tissues suggest that the hNOG mice allow for sufficient development of human cells to make the study of HIV-1 pathogenesis possible.

Both R5- and X4-tropic HIVs efficiently infect and replicate in hNOG mice

In our preliminary study, using low and high doses of challenge virus, no viral infection was detected in any of the virus-inoculated hNOG mice at 7 days after infection, while some showed detectable plasma viral loads at 14 days (data not shown). Then, we prepared 16 hNOG mice that received transplants of stem cells and inoculated them with a high dose of R5-tropic HIV-1$_{JRCSF}$ (65 000 TCID$_{50}$) and X4-tropic SHIV-C2/1 (50 000 TCID$_{50}$) intravenously through the tail vein at 102 to 132 days after transplantation. Upon HIV-1$_{JRCSF}$ infection, viral copy numbers in plasma rose to a level of 1.6×10^5 to 5.8×10^5 copies/mL (n = 4) on day 33 and 2.0×10^5 to 4.7×10^5 copies/mL on day 43 (n = 4) (Figure 4A). Moreover, for SHIV-C2/1 infection, viral copy numbers in plasma were 1.6×10^3 to 3.2×10^5 copies/mL on day 18 (n = 4) and reached 5.4×10^4 to 1.1×10^5 copies/mL on day 42 (n = 4; Figure 4B). In these mice, no significant decline in the CD4/CD8 ratio was observed throughout entire period of follow-up for the R5-tropic virus infection, while CD4$^+$ cell decline was detected for the X4-tropic virus infection on day 42 after infection (P = .044) but not on day 18 after infection (Figure 4C). Four mice that did not receive transplants of human stem cells showed no detectable levels of plasma viral load (less than 500 copies/mL) following HIV/SHIV inoculation (data not shown).

To confirm HIV infection, we used immunohistochemistry to detect the presence of the p24 antigen of the HIV-1 Gag protein in various tissues of mice showing viremia. p24$^+$ cells were clearly identified in the spleen, LN, and lungs (Figure 4D), which include macrophage-like cells.

Different distributions of R5- and X4-tropic viruses in lymphoid tissues

A number of mice (14) were further analyzed for HIV-1 infection on days 126 to 146 after transplantation with a low dose (200 TCID$_{50}$) or a high dose (65 000 TCID$_{50}$) of R5-tropic HIV-1$_{JRCSF}$ and a low dose (180 TCID$_{50}$) or a high dose (20 000 TCID$_{50}$) of X4-tropic HIV-1$_{MNp}$. Consequently, 2 of the 4 mice given a low

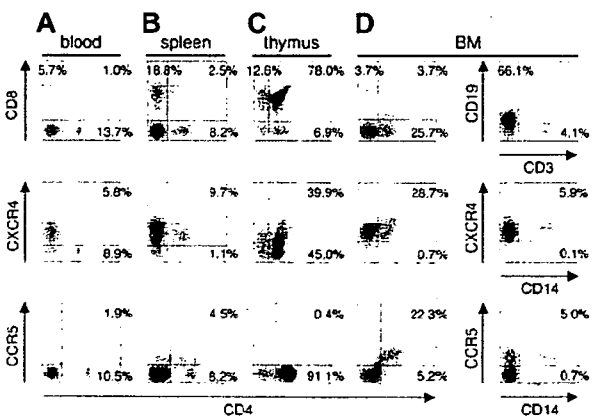

Figure 3. Surface expression of HIV-1 coreceptors on CD4$^+$ cells in various organs of mice 4 months after transplantation. A representative FACS profile of human CXCR4 and CCR5 on CD4$^+$ cells shows the existence of CXCR4$^+$CD4$^+$ and CCR5$^+$CD4$^+$ cells in blood (A), spleen (B), and BM (D), but no CCR5$^+$CD4$^+$ cells in the thymus (C). BM results show that many CD4$^+$ cells are neither CD3$^+$ T cells nor CD14$^+$ monocytes. A gate was set on the human CD45$^+$ population.